

1 **CCER valuation under emission uncertainty: a dual**
2 **framework of compliance optimization and regime-**
3 **switching GBM¹**

4 Hua Tang^{1,2}, Yue Liu³, Jiayi Wang³, Jiawen Liu³, Wangfei Luo⁴, Tianbai Wang⁵

5 (1 School of Management, Jiangsu University, Zhenjiang, 212013, Jiangsu, PR China; 2 Business
6 School of Wenzhou University, Wenzhou City, 325035, Zhejiang, PR China; PR China; 3 School of
7 Finance and Economics, Jiangsu University, Zhenjiang, 212013, Jiangsu, PR China; 3 School of
8 Finance and Economics, Jiangsu University, Zhenjiang, 212013, Jiangsu, PR China; 4 School of
9 Electrical and Information Engineering, Jiangsu University, Zhenjiang 212013, PR China; 5 China
10 School of Banking and Finance UIBE, University of International Business and Economics,
11 Beijing, 100029, PR China)

12

13 Supported by the grant from the Major Program of the National Social Science Fund of China
14 (22&ZD136).

¹ Corresponding author' email address: Jiayi Wang: 15139253806@163.com
Other co-authors' email addresses: Hua Tang : tanghua@edu.wzu.cn ; Yue Liu: liuy0080@e.ntu.edu.sg; Jiawen
Liu: 18951131673@163.com; Wangfei Luo: lwf20041225@126.com; Tianbai Wang: postboxfly@163.com

15 **CCER valuation under emission uncertainty: a dual**

16 **framework of compliance optimization and regime-**

17 **switching GBM**

18 **Abstract:** This paper develops an integrated framework to value China Certified Emission
19 Reductions (CCER) in the context of the national emissions trading system. At the micro level, we
20 refine the income approach by endogenizing firms' CCER purchase decisions under emission
21 uncertainty, offset caps and residual value risk, deriving a closed-form marginal willingness-to-pay
22 schedule linked to firm-specific emission distributions, allowance allocations and policy parameters.
23 At the macro level, we model carbon prices with a three-regime switching geometric Brownian
24 motion calibrated to Beijing carbon market and electricity data, and price CCER as a real-option-like
25 asset with state-dependent CEA-CCER spreads and guarantee-type payoffs. Comparing the two
26 layers, we show how income-based benchmarks and regime-switching option values differ yet can
27 be aligned to inform CCER pricing, contract design and policy reform in China's carbon market.

28

29 **Keywords:** CCER valuation; Carbon assets; Income approach; Regime-switching GBM; Real
30 options.

31

32

33

34

35

36 1 Introduction

37 China's national carbon emission trading system incorporates the China Certified Emission
38 Reduction (CCER) mechanism as a key supplementary instrument for achieving carbon peaking and
39 neutrality targets at reduced costs. Regulated enterprises may substitute CCER for Carbon Emission
40 Allowances (CEA) up to specified proportions when offsetting verified emissions, which should in
41 theory lower aggregate abatement costs while channeling investment toward low-carbon projects. Yet
42 CCER's actual economic value emerges from the interplay of multiple factors: firm-level emission
43 uncertainty, quota allocation methodologies, caps on offsetting ratios, policy-driven sunset clauses
44 governing CCER eligibility, and carbon market prices that swing with macroeconomic cycles and
45 regulatory shifts. These institutional and market features reveal that CCER functions neither as a
46 riskless compliance instrument nor as a straightforward derivative of CEA prices; both enterprises
47 and regulators require valuation frameworks capable of reconciling micro-level compliance
48 incentives with macro-level price movements.

49 Current CCER valuation practices display fragmentation across two dimensions. Income
50 approach studies concentrate on the expected cost savings CCER delivers relative to CEA, yet these
51 analyses commonly take CCER purchase volumes as given and overlook maturity and residual value
52 risks, thereby constraining their capacity to represent firms' actual procurement decisions under
53 uncertainty. Market approach studies deploy stochastic models for carbon prices but frequently treat
54 CCER as a scaled replica of CEA, failing to explicitly embed compliance constraints, offset ratios,
55 or policy validity windows. A disconnect has thus emerged between enterprise-centered analysis that
56 proves intuitive but static and market-centered modeling that remains dynamic yet weakly anchored
57 to the compliance architecture. This paper seeks to close that gap by developing an integrated

58 framework: it merges a micro-level income approach grounded in firms' optimal CCER demand with
59 a macro-level market approach that captures CEA and CCER price evolution via regime switching
60 (Hussain et al., 2021) and geometric Brownian motion (Li, W. et al., 2021; Liu, Y. et al., 2023a; Liu,
61 Y. et al., 2023b), pricing CCER as a real-option-like asset.

62 From this integrated perspective, the paper advances three principal innovations. First, at the
63 micro level, it refines the income approach by endogenizing CCER purchase quantities as solutions
64 to compliance cost minimization problems under stochastic emissions, regulatory ceilings, and
65 uniform residual values. This yields a closed-form marginal willingness-to-pay curve that directly
66 links firm-specific emission distributions, quota allocations, and policy parameters to CCER
67 valuation. Second, at the macro level, the paper introduces a three-state regime-switching geometric
68 Brownian motion model calibrated using Beijing carbon market data and electricity consumption
69 growth patterns. It jointly models CEA and CCER prices under regime-dependent drift rates,
70 volatilities, and spread ratios, valuing CCER through discounted risk-neutral expectations based on
71 guarantee-type payoffs that reflect compliance substitutability and residual value floors. Third, the
72 paper juxtaposes micro- and macro-level findings, employing shared calibration inputs such as
73 expected CEA settlement prices and CCER residual values to conduct a consistent cross-comparison
74 of valuation outcomes. Results demonstrate that the income approach's benchmark value and regime-
75 switching real option valuation together furnish a foundation for CCER pricing, contract design, and
76 policy formulation.

77 **2 Literature review**

78 We take the literature review via two aspects, one is about carbon asset, another is about asset

79 pricing especially for intangible assets.

80 2.1 Review on the researches about carbon asset

81 Recent work on carbon assets has started to connect climate policy, corporate decision-making,
82 and financial market behavior, shedding light on both transition risks and emerging valuation
83 challenges. Research at the sectoral and policy level shows that concentrated ownership of power-
84 sector assets vulnerable to stranding creates vested interests capable of slowing or blocking ambitious
85 climate measures, pointing to governance obstacles and distributional tensions in decarbonization
86 pathways (Chevallier et al., 2021; von Dulong, 2023). Analyses of corporate carbon footprints across
87 complete value chains find that embedded emissions in listed firms vary dramatically between
88 upstream and downstream operations, altering how investors assess risk exposure and meet disclosure
89 obligations (Langley et al., 2021; Zhang et al., 2023). Firm-level data indicate that equity markets
90 now price corporate carbon emissions more systematically, with valuations reflecting both total
91 emissions and the perceived credibility of decarbonization plans (Zhang, 2025; Chen and Lai, 2025).
92 On the asset-pricing front, researchers increasingly model carbon allowances and credits as
93 contingent claims: option frameworks price carbon assets and support digital tools for dynamic
94 hedging and project evaluation (Liu et al., 2022), while real-options techniques measure the economic
95 value of operational choices such as continuing or shutting down emission-intensive power plants
96 under tightening carbon limits (Liu et al., 2021). Where macro-finance meets climate, carbon pricing
97 emerges as a driver of structural change toward greener growth trajectories, redirecting capital flows
98 from high-carbon sectors (Langley et al., 2021; Mengesha and Roy, 2025), yet climate and policy
99 uncertainty propagate forcefully across energy and carbon markets, with asymmetric causal
100 connections running among economic policy uncertainty, oil price volatility, clean energy indices,

101 carbon futures and green bonds (Wang X. et al., 2022; Siddique et al., 2023). Empirical studies further
102 reveal pronounced spillovers linking fossil fuel, renewable and carbon markets during overlapping
103 climate and energy shocks, implying that carbon assets sit within larger energy-finance networks
104 rather than standing alone (Su et al., 2023; Dong and Yoon, 2023). Meanwhile, the relaunch of China's
105 CCER market has spurred methodological and project-level advances: feasibility assessments of
106 methane-reduction approaches in oil and gas production highlight a new category of carbon assets
107 with substantial mitigation leverage (Wang et al., 2025), and integrated carbon asset management
108 platforms and trading tactics seek to help listed enterprises revalue assets and pursue sustainable
109 development goals (Chen and Lai, 2025). Taken together, these studies suggest that carbon assets are
110 shifting from a narrow compliance tool into a diverse financial and strategic asset class whose worth
111 hinges on policy architecture, technology trajectories, cross-market linkages and firm-level
112 organizational capacity (Chevallier et al., 2021; Liu et al., 2022; Mengesha and Roy, 2025). Beyond
113 energy and finance, valuation-relevant impacts of carbon-related assets and practices now extend into
114 material-production industries including agriculture and chemicals, covering soil carbon
115 sequestration, inorganic soil carbon behavior, and biochar-derived carbon materials (Nazir et al.,
116 2023; Raza et al., 2024; Mahmood et al., 2025).

117 2.2 Review on the researches about intangible asset pricing

118 A growing body of research on intangible asset pricing examines how non-physical drivers such
119 as information, expectations, environmental performance and intellectual capital increasingly shape
120 asset values. At the measurement and reporting level, surveys and meta-analyses point to persistent
121 gaps between the economic significance of intangibles and their treatment in financial statements,
122 documenting conceptual and empirical obstacles in valuing items such as R&D, data, and

123 organizational capital (Van Criegingen et al., 2022; Jeny and Moldovan, 2022; Barker et al., 2022).
124 Firm-level studies build on these observations to show that intangible resources can forecast future
125 performance and ought to be priced by investors, with deep learning models extracting value-relevant
126 signals from complex intangible asset profiles (Pechlivanidis et al., 2022). Related work broadens the
127 concept of intangibles to include environmental attributes: carbon emissions and carbon risk enter
128 asset pricing models as non-traditional factors, with mounting evidence that emissions and climate
129 exposures affect stock returns and capital costs, especially in emerging markets (van Benthem et al.,
130 2022; Wang H. et al., 2022; Bolton and Kacperczyk, 2024). Time-varying investor preferences for
131 green attributes and evolving policy signals further influence how environmental performance gets
132 rewarded in asset prices, suggesting that such performance has itself become a priced intangible
133 (Dutta, 2022; Alessi et al., 2023). Where macro-policy meets asset valuation, studies of risk-adjusted
134 carbon prices and retrospective evaluations of carbon pricing schemes reveal that expectations about
135 future regulation and abatement costs embed themselves into long-run asset values, effectively
136 converting regulatory trajectories into a form of priced intangible risk (Van den Bremer and Van der
137 Ploeg, 2021; Green, 2021). On the methodological front, advances in behavioral and computational
138 finance demonstrate that even nominal price illusions and data monetization practices introduce new
139 intangible dimensions into pricing: behavioral biases in nominal valuation distort asset prices in ways
140 traditional factors miss, while datasets themselves become tradable intangible assets whose prices
141 can be learned via deep learning-based monetization frameworks (Yang and Yang, 2022; Hao et al.,
142 2025). Taken together, this literature argues that modern asset pricing must systematically incorporate
143 a wide spectrum of intangibles spanning accounting-based intellectual capital, proprietary data,
144 environmental quality and policy expectations, deploying richer models and machine learning

145 techniques to connect these largely off-balance-sheet attributes to observed returns (Van Crikingen
146 et al., 2022; Pechlivanidis et al., 2022; Alessi et al., 2023).

147 These studies collectively demonstrate that carbon assets and other intangibles are increasingly
148 priced through their interactions with policy, firm behavior and market expectations, yet existing
149 research tends to separate micro compliance analyses from macro market models. Drawing on these
150 insights, this paper treats CCER as a carbon-related intangible asset and constructs an integrated
151 valuation framework that connects optimal firm-level CCER demand under emission and policy
152 uncertainty with regime-switching GBM-based pricing of CEA and CCER, bridging income-based
153 and market-based perspectives to inform CCER pricing, contract design and policy.

154 **3 Micro-level CCER valuation:from the firms' perspective**

155 **3.1 Theoretical analysis and model construction**

156 This section constructs an improved CCER valuation model grounded in optimal enterprise
157 purchasing decisions under emission uncertainties, regulatory constraints, and policy-induced
158 invalidation risk. Unlike earlier discrete and continuous distribution models where CCER quantity
159 enters exogenously and unit value represents average cost savings per ton, the present framework
160 endogenizes purchased CCER quantity as the solution to a cost minimization problem and derives
161 the associated willingness to pay as a theoretically grounded estimate of marginal value. This
162 approach preserves the intuitive cost-difference logic inherent in the income method while directly
163 tying CCER value to firm-specific emission risk, incorporating residual value and the potential for
164 excess CCER to lose validity after the compliance window, and permitting heterogeneous enterprise
165 characteristics such as size, quota allocation and volatility to generate differentiated CCER

166 valuations.

167 We consider a representative compliance enterprise i facing uncertain annual carbon emissions
168 in the target year (for instance, 2024). Let E denote its random annual emissions (tonnes of CO2
169 equivalent). Consistent with the empirical setting in the previous section, E is modeled from
170 historical data (2017–2023) and is assumed to follow a continuous distribution with mean μ_E and
171 variance σ_E^2 , with cumulative distribution function $F_E(\cdot)$ well-defined; in applications a normal or
172 lognormal specification can be used, or an empirically estimated non-parametric distribution.

173 The enterprise holds or expects to receive an annual allocation of carbon emission allowances
174 (CEA) denoted by A , and may purchase a quantity Q of CCER to offset emissions in the same
175 compliance period. The maximum proportion of emissions that can be offset with CCER is capped at
176 α (5% in the Chinese system), which implies an upper bound $Q \leq Q^{max}$, where Q^{max} can be set as
177 $\alpha\mu_E$ or, more conservatively, as $\alpha(\mu_E + z\sigma_E)$ for a chosen safety quantile z . Throughout the analysis
178 we treat Q as a continuous decision variable in $[0, Q^{max}]$.

179 At the beginning of the compliance period (or at an intermediate time before the deadline), the
180 firm chooses Q and pays $p_C Q$, where p_C is the unit market price of CCER. We assume that the
181 CEA price at the time of final compliance is stochastic but that the firm can form an expectation \bar{p}_A
182 of the average marginal cost of acquiring additional CEA close to the settlement date, inferred from
183 historical trading data or from a separate market-approach model (e.g., GBM or LSTM). The
184 regulatory frame-work typically stipulates a penalty F per tonne of uncovered emissions; for
185 analytic clarity we assume $F \geq \bar{p}_A$, so that a rational firm will always purchase CEA to achieve full
186 coverage before paying penalties, and compliance behavior can be summarized as ‘buy CEA until the
187 emission shortfall is fully covered’.

188 Given a realization of E , the firm's compliance balance at the end of the period is $A + Q$. If
 189 $E > A + Q$, the firm must purchase additional CEA on the spot market to cover the shortfall $E -$
 190 $A - Q$ at expected marginal cost $\bar{p}_A(E - A - Q)$, ignoring second-order price feedback from
 191 individual trades. If instead $E < A + Q$, the firm ends the period with surplus compliance assets $A +$
 192 $Q - E$. Because CCER eligibility in the Chinese national trading system is subject to strict temporal
 193 limitations (for example, credits registered before March 14, 2017 are usable only until December 31,
 194 2024 and CCER trading effectively ceases after the compliance submission deadline), surplus CCER
 195 face significant expiration and liquidity risks, whereas surplus CEA generally remain valid and
 196 tradable in subsequent periods or can be sold back to the market.

197 To capture these asymmetries while keeping the model tractable, we postulate that surplus
 198 compliance assets at the end of the period are valued at a residual price v_C^{res} . A more detailed
 199 specification could distinguish between surplus CEA and CCER, for example assigning CEA a
 200 residual value close to \bar{p}_A and CCER a value $(1 - \theta)\lambda p_C$ based on a survival probability $(1 - \theta)$
 201 and a resale discount factor $\lambda \in [0,1]$ in voluntary markets. For parsimony, we aggregate these effects
 202 into a single effective residual value v_C^{res} , interpreted as the expected liquidation value per tonne of
 203 surplus compliance asset, net of policy invalidation and market illiquidity; typically $v_C^{res} < \bar{p}_A$ and,
 204 for CCER approaching their sunset date, it can be substantially lower.

205 Under these assumptions, for a given CCER purchase quantity Q and a particular realization of
 206 emissions E , the firm's random total cost of compliance can be written as

$$207 \quad \text{TC}(Q; E) = p_C Q + \bar{p}_A(E - A - Q)_+ - v_C^{res}(A + Q - E)_+, \quad (3.1)$$

208 where $(x)_+ = \max\{x, 0\}$. Here $p_C Q$ is the certain upfront cost of purchasing Q tonnes of CCER,
 209 $\bar{p}_A(E - A - Q)_+$ is the cost of "filling the gap with CEA" when realized emissions exceed $A + Q$,

210 and $-\nu_C^{res}(A + Q - E)_+$ reflects the residual value of surplus compliance assets when $E < A + Q$.

211 Given CCER purchase quantity Q , the firm's expected total compliance cost is

212
$$\mathbb{E}[\text{TC}(Q; E)] = p_C Q + \mathbb{E}[\bar{p}_A (E - A - Q)_+] - \mathbb{E}[\nu_C^{res}(A + Q - E)_+], \quad (3.2)$$

213 where the expectation is taken over $E \sim f_E(e)$. The firm's decision problem is

214
$$Q^* = \arg \min_{0 \leq Q \leq Q^{\max}} \mathbb{E}[\text{TC}(Q; E)], \quad (3.3)$$

215 which formalizes, within the income-approach framework, the strategic decision of 'how many
216 CCER to buy' under emission and price uncertainty.

217 To derive the first-order condition for an interior solution, differentiate (3.2) with respect to Q .

218 Since $\text{TC}(Q; E)$ depends on Q only through $p_C Q$ and the positive-part terms, and $(E - A -$
219 $Q)_+$, $(A + Q - E)_+$ are almost everywhere differentiable in Q , we
220 have $\frac{\partial}{\partial Q} (E - A - Q)_+ = -1_{\{E > A + Q\}}$ and $\frac{\partial}{\partial Q} (A + Q - E)_+ = 1_{\{E < A + Q\}}$, where $1_{\{\cdot\}}$ denotes the
221 indicator function. Substituting and using linearity of expectation gives

222
$$\begin{aligned} \frac{d}{dQ} \mathbb{E}[\text{TC}(Q; E)] &= p_C + \mathbb{E}[-\bar{p}_A 1_{\{E > A + Q\}} - \nu_C^{res} 1_{\{E < A + Q\}}] \\ &= p_C - \bar{p}_A \mathbb{P}(E > A + Q) - \nu_C^{res} \mathbb{P}(E < A + Q), \end{aligned} \quad (3.4)$$

224 where we used $\mathbb{E}[1_{\{E > A + Q\}}] = \mathbb{P}(E > A + Q)$ and $\mathbb{E}[1_{\{E < A + Q\}}] = \mathbb{P}(E < A + Q)$. The second term
225 represents the expected marginal saving in CEA "gap-filling" cost, and the third term captures the
226 change in expected residual value from buying one more tonne of CCER.

227 Setting (3.4) equal to zero at Q^* yields

228
$$p_C = \bar{p}_A \mathbb{P}(E > A + Q^*) + \nu_C^{res} \mathbb{P}(E < A + Q^*). \quad (3.5)$$

229 For a continuous emission distribution we have $\mathbb{P}(E > A + Q^*) + \mathbb{P}(E < A + Q) \approx 1$.

230 Rearranging (3.5) gives the key pricing relation

231
$$\underbrace{p_C}_{\substack{\text{CCER unit price at } Q^* \\ (\text{marginal willingness-to-pay})}} = \underbrace{v_C^{res}}_{\substack{\text{residual value benchmark} \\ \text{when CCER mainly end as surplus}}} +$$

232
$$\underbrace{(\bar{p}_A - v_C^{res})}_{\substack{\text{compliance-use premium} \\ \text{over pure residual value}}} \underbrace{\mathbb{P}(E > A + Q^*)}_{\substack{\text{probability of an emission shortfall} \\ \text{after buying } Q^* \text{ tonnes of CCER}}}$$

233 (3.6)

234 The marginal willingness-to-pay at Q^* is thus a weighted average of the expected marginal CEA
 235 cost \bar{p}_A and the residual value v_C^{res} , with the weight on \bar{p}_A given by the shortfall probability
 236 $\mathbb{P}(E > A + Q^*)$. When this probability is high, p_C is close to \bar{p}_A ; when it is low, p_C moves toward
 237 v_C^{res} .

238 To obtain an explicit pricing formula, assume $E \sim \mathcal{N}(\mu_E, \sigma_E^2)$, with (μ_E, σ_E) estimated from
 239 historical firm-level data. The shortfall probability can then be expressed via the standard normal
 240 CDF $\Phi(\cdot)$ as

241
$$\mathbb{P}(E > A + Q) = 1 - \Phi\left(\frac{A+Q-\mu_E}{\sigma_E}\right).$$
 (3.7)

242 Substituting (3.7) into (3.6) yields the central CCER price-quantity relation

243
$$\underbrace{p_C^*(Q)}_{\substack{\text{firm-level marginal} \\ \text{willingness-to-pay at } Q}} = \underbrace{v_C^{res}}_{\substack{\text{residual value in} \\ \text{surplus states}}} + \underbrace{(\bar{p}_A - v_C^{res})}_{\substack{\text{incremental value of CCER} \\ \text{as a compliance instrument}}} \underbrace{\left[1 - \Phi\left(\frac{A+Q-\mu_E}{\sigma_E}\right)\right]}_{\substack{\text{probability of a shortfall} \\ \text{after purchasing } Q \text{ tonnes of CCER}}}$$
 (3.8)

244 For small Q such that $A + Q \ll \mu_E$, the standardized term $(A + Q - \mu_E)/\sigma_E$ is very negative,
 245 $\Phi(\cdot)$ is close to 0, and the shortfall probability is close to 1, so $p_C^*(Q) \approx \bar{p}_A$ and CCER are almost
 246 fully valued at the expected marginal CEA price; as Q increases and $A+Q$ approaches or exceeds
 247 μ_E , the shortfall probability declines and $p_C^*(Q)$ decreases smoothly from \bar{p}_A toward v_C^{res} ,
 248 reflecting the transition from ‘insurance against costly shortfalls’ to ‘potentially stranded surplus
 249 assets’.

252 Thus, (3.8) can be interpreted as a firm-level demand curve for CCER: for each $Q \in [0, Q^{\max}]$,
253 it gives the marginal price that leaves the firm indifferent between buying an additional tonne of
254 CCER and relying instead on spot CEA purchases or accepting surplus risk. Coupled with (3.3), the
255 most relevant income-based valuations at the firm level are $p_C^*(Q^*)$ (marginal value at the optimum)
256 and $p_C^*(Q^{\max})$ (marginal value when the regulatory offset ratio is fully used). Aggregating such firm-
257 specific marginal values, for example via emission-weighted averages, yields a market-level
258 theoretical CCER price range under the improved income-approach framework.

259 In implementation: (1) For each firm, estimate (μ_E, σ_E) from historical emissions and determine
260 its expected allowance allocation A under national ETS rules, then compute $Q^{\max} = \alpha\mu_E$. (2)
261 Specify \bar{p}_A from observed or modeled CEA prices at compliance, and calibrate v_C^{res} using policy
262 information on CCER validity and expected liquidity. (3) For each Q on a grid in $[0, Q^{\max}]$, compute
263 $\mathbb{P}(E > A + Q)$ via (3.7) and then $p_C^*(Q)$ via (3.8). (4) Solve (3.3) for Q^* , obtain $p_C^*(Q^*)$ or
264 $p_C^*(Q^{\max})$, and aggregate across firms to form a market reference price.

265 3.2 Numerical implementation and discussion on the results

266 The numerical implementation proceeds as follows (the Matlab implementation for the income-
267 approach model is provided in Appendix B). The model first sets the key global parameters $\alpha =$
268 0.05 , $\bar{p}_A = 115$ CNY/t and $v_{res} = 30$ CNY/t, where α is the maximum CCER offset ratio, \bar{p}_A is
269 the expected marginal CEA settlement price, and v_{res} is the residual (floor) value of CCER.
270 Historical daily CEA and CCER prices from the Word file are read into the program but are used only
271 as background, while the pricing model itself is calibrated directly using the fixed values of \bar{p}_A and
272 v_{res} .

273 Firm-level emission data are then imported separately for low-emission firms (Table 2) and

274 normal-emission firms (Table 3). For each firm, the Appendix A provides E_{upper} , E_{mid} and E_{lower}
 275 for annual emissions. The code sets $\mu_E = E_{mid}$ as the firm's expected emissions and, assuming
 276 (E_{lower}, E_{upper}) is roughly a 90% confidence interval, approximates the standard deviation by $\sigma_E \approx$
 277 $(E_{upper} - E_{lower})/(2z_{0.95})$ with $z_{0.95} \approx 1.64$, imposing $\sigma_E \geq 10^{-6}$ to avoid degeneracy. The
 278 allowance allocation is set equal to expected emissions, $A = \mu_E$, and the maximum CCER usage is
 279 $Q_{max} = \alpha \mu_E$.

280 Based on these inputs, the firm-specific marginal willingness-to-pay function for CCER is
 281 implemented as

$$282 p_c^*(Q) = v_{res} + (\bar{p}_A - v_{res}) \left[1 - \Phi \left(\frac{A+Q-\mu_E}{\sigma_E} \right) \right],$$

283 where $\Phi(\cdot)$ is the standard normal cumulative distribution function. In the code this is written as a
 284 vectorized anonymous function *pc_fun* using *normcdf*. For each firm, the program evaluates
 285 $p_c^*(Q)$ at $Q = 0$, $Q = Q_{max}$ and $Q = Q^*$, where Q^* is obtained by minimizing the expected total
 286 compliance cost over $Q \in [0, Q_{max}]$,

$$287 \mathbb{E}[TC(Q; E)] = p_c^*(Q)Q + \bar{p}_A \mathbb{E}[(E - T)_+] - v_{res} \mathbb{E}[(T - E)_+], \quad T = A + Q,$$

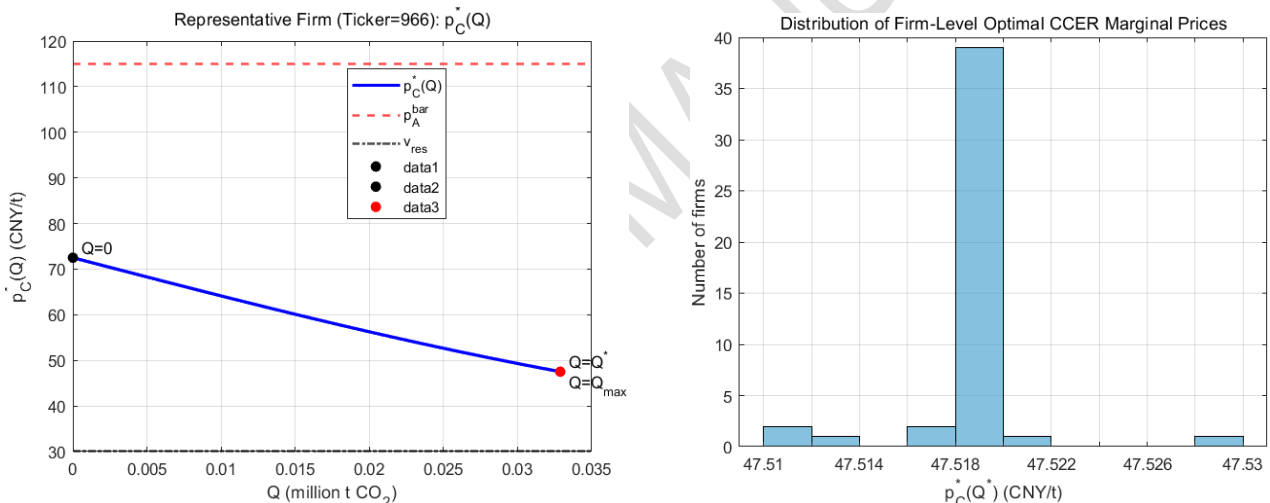
288 with $(x)_+ = \max\{x, 0\}$. Under the normality assumption for E , the expectations $\mathbb{E}[(E -$
 289 $T)_+]$ and $\mathbb{E}[(T - E)_+]$ have closed-form expressions involving the standard normal *pdf* and *cdf*,
 290 which are implemented in an auxiliary function *ETC_single*. The scalar optimization is carried out
 291 using the Matlab routine *fminbnd*, yielding the optimal Q^* and the associated marginal price $p_c^*(Q^*)$
 292 for each firm.

293 Using this procedure, the program computes for all 46 firms the mean emissions μ_E , emission
 294 volatility σ_E , maximum CCER use Q_{max} and the model-implied marginal CCER prices at $Q =$
 295 0 , $Q = Q_{max}$ and $Q = Q^*$. The numerical results show that: (1) for all firms, the predicted marginal
 296 price at zero CCER usage is identical and equals $p_c^*(0) = 72.50$ CNY/t. This is because at $Q = 0$

297 we have $T = A = \mu_E$, so $\Phi(0) = 0.5$ and $p_C^*(0) = v_{res} + (\bar{p}_A - v_{res})(1 - \Phi(0)) = 30 + (115 -$
 298 $30) \times 0.5 = 72.5$. (2) When firms use CCER up to the policy cap $Q_{max} = \alpha\mu_E$, the marginal
 299 willingness-to-pay falls for all firms to approximately $p_C^*(Q_{max}) \approx 47.52$ CNY/t, because
 300 additional CCERs raise the total compliance position $T = A + Q$ and reduce the probability that the
 301 firm ends up short and needs to settle at the higher CEA price \bar{p}_A . (3) The optimization results show
 302 that for every firm in the sample, the cost-minimizing choice is $Q^* = Q_{max}$, so $p_C^*(Q^*) =$
 303 $p_C^*(Q_{max}) \approx 47.52$ CNY/t.

304 The program also computes emission-weighted average theoretical CCER prices across all firms
 305 (using μ_E as weights). The results are (CNY/t) : Mean $p_C^*(Q = 0) = 72.50$, Mean $p_C^*(Q =$
 306 $Q_{max}) = 47.52$, Mean $p_C^*(Q = Q^*) = 47.52$.

307



308
 309 Figure 1: Representative-firm marginal CCER pricing curve and cross-sectional distribution of
 310 optimal marginal CCER prices

311 Because all firms optimally choose $Q^* = Q_{max}$, the average optimal marginal price coincides
 312 with the marginal price at the cap. The left graph in Fig 1 illustrates the marginal willingness-to-pay
 313 curve $p_C^*(Q)$ for a representative firm, chosen in the code as the one whose expected emissions are
 314 closest to the sample median, namely the firm with ticker 966, for which (t CO2) $\mu_E = 657,528$, $\sigma_E =$
 315 $40,093.29$, $A = 657,528$, $Q_{max} = 32,876.40$. The horizontal axis of the left graph in Fig 1 plots Q
 316 (in million tonnes CO2) from 0 to Q_{max} , and the vertical axis reports $p_C^*(Q)$ in CNY/t. The curve

317 starts at $p_c^*(0) = 72.50$ CNY/t and monotonically declines to $p_c^*(Q_{max}) \approx 47.52$ CNY/t as
 318 Q increases, with two horizontal reference lines at $\bar{p}_A = 115$ CNY/t and $v_{res} = 30$ CNY/t. The
 319 points $Q = 0$, $Q = Q_{max}$ and $Q = Q^*$ are highlighted on the curve; since for this firm
 320 $Q^* = Q_{max} = 32,876.40$ t CO₂, the last two coincide and $p_c^*(Q^*) = p_c^*(Q_{max}) \approx 47.52$ CNY/t. The
 321 right graph in Fig 1 summarizes the cross-sectional distribution of $p_c^*(Q^*)$ for all 46 firms. The
 322 horizontal axis is $p_c^*(Q^*)(\text{CNY/t})$ and the vertical axis is the number of firms. The descriptive
 323 statistics are: $\min p_c^*(Q^*) = 47.51$ CNY/t, $\max p_c^*(Q^*) = 47.53$ CNY/t, mean = 47.52 CNY/t ,
 324 median = 47.52 CNY/t, std. dev. ≈ 0.00 CNY/t, indicating an extremely concentrated distribution.

325 Overall, the numerical results yield three main conclusions. First, when firms hold allowances
 326 equal to their expected emissions, the initial marginal value of CCER at zero usage is exactly halfway
 327 between the residual CCER value and the expected CEA price, that is $p_c^*(0) = \frac{1}{2}(\bar{p}_A + v_{res}) =$
 328 72.5 CNY/t. Second, as firms increase CCER usage up to the regulatory cap, their marginal
 329 willingness-to-pay declines to about 47.52 CNY/t, but remains well above the residual value of
 330 30 CNY/t, which supports a non-trivial economic value of CCER under the given market conditions.
 331 Third, under the current parameterization all firms optimally choose $Q^* = Q_{max}$, so the cross-sectional
 332 dispersion of $p_c^*(Q^*)$ is negligible, as illustrated by the right graph in Fig 1.

333 These findings highlight both the internal consistency and the limitations of the current
 334 calibration. The income-approach model delivers a transparent relationship between the CEA price,
 335 the CCER residual value and firms' optimal CCER demand, while the near-degeneracy of the cross-
 336 sectional distribution suggests that richer heterogeneity in allowance allocation rules, emission
 337 uncertainty and firm-specific constraints, or relaxing the assumption $A = \mu_E$ for all firms, would
 338 generate a wider and more realistic spread of $p_c^*(Q^*)$ than that shown in the right graph in Fig 1.

339 **4 Macro-level CCER valuation: from the market's perspective**

340 In this section, we employ the market approach to model carbon prices through a regime-
341 switching geometric Brownian motion (GBM). Compared to a single-regime GBM, this framework
342 is capable of capturing structural shifts in economic activity, energy demand, and regulatory policies,
343 thereby depicting the nonlinear, state-dependent dynamics of CEA and CCER. We treat CEA prices
344 as the underlying asset in a risk-neutral regime-switching GBM and value CCER as a real option,
345 while considering observable price boundaries, offset substitutability with CEA, and policy-mandated
346 offset ratio constraints.

347 **4.1 Theoretical analysis of the value-relevance of CCER and CEA**

348 For compliance enterprises, one unit of CCER can either offset one ton of verified emissions on
349 the compliance date or be sold on the secondary market before its expiration, thus representing a
350 flexible right. Holding CCER units with an expiration date of T at time zero grants the holder the
351 right to choose between compliance use and market sale, with the higher benefit prevailing at or
352 before time T . Let P_t^A and P_t^C be CEA and CCER prices at time t , and r the continuously
353 compounded risk-free rate. Empirically P_t^C is usually below P_t^A and bounded below by a residual
354 value ν_{res} , so a basic restriction is $0 \leq \nu_{res} \leq P_t^C \leq P_t^A$.

355 We approximate the marginal compliance value of one CCER at T by an increasing function
356 $f(P_T^A)$ of the settlement CEA price. Under full substitutability and ignoring firm-specific
357 constraints, we use $f(P_T^A) = \min\{P_T^A, \bar{p}_A^{max}\}$, where \bar{p}_A^{max} is an effective cap on the CEA settlement
358 price. The time-zoo CCER value under the risk-neutral measure \mathbb{Q} is $V_0^C = e^{-rT} \mathbb{E}^{\mathbb{Q}}[f(P_T^A)]$, which
359 is constrained to satisfy $\nu_{res} \leq V_0^C \leq V_0^A$, where V_0^A is the risk-neutral value of one CEA unit.

360 Calibration of $f(\cdot)$ is chosen so that the implied ratio $\theta_t = P_t^C/P_t^A$ lies in the empirical band $\underline{\theta} \leq$
361 $\theta_t \leq \bar{\theta}$.

362 In the Beijing CCER market, Table 1 indicates that θ_t is typically between 0.56 and 1.08, with
363 $P_t^C \leq P_t^A$ and a common range around 0.6 to 0.7. To reflect this structure, we specify a state-
364 dependent pricing kernel $P_t^C = \theta(\alpha_t)P_t^A$, where α_t is an unobserved economic regime and $\theta(\alpha_t)$
365 is the CCER-CEA price ratio in regime α_t . Given the regime-switching process for P_t^A , CCER
366 prices are thus driven jointly by P_t^A and the regime index α_t .

367 Regime uncertainty is modeled by a continuous-time finite-state Markov chain $(\alpha_t)_{t \geq 0}$ with
368 state space $\mathcal{M} = \{e_1, e_2, \dots, e_m\}$, representing different macro or regulatory conditions. For more
369 details of Markov chain's modelling and applications, we refer to (Zheng et al., 2020; Ni et al., 2024;
370 Xu et al., 2024). The "regime" can be understood as a combination of high, medium, and low levels
371 of temperature and industrial activity, or more broadly as a state defined by temperature, coal prices,
372 industrial added value growth rates, and regulatory policy dynamics. This Markov chain determines
373 the drift rate, volatility, and spread ratio $\theta(\cdot)$ of the CEA price process, and therefore transmits
374 regime shifts into CCER valuation.

375 4.2 Modeling CEA and CCER prices with regime-switching geometric Brownian
376 motion

377 We now specify a regime-switching geometric Brownian motion (GBM) for CEA and CCER
378 prices. Let $(B_t)_{t \geq 0}$ be a standard Brownian motion and $(\alpha_t)_{t \geq 0}$ a continuous-time Markov chain
379 on $\mathcal{M} = \{e_1, \dots, e_m\}$ with generator $Q = (q_{ij})_{1 \leq i, j \leq m}$, where $q_{ij} \geq 0$ for $i \neq j$ and $q_{ii} = -\sum_{j \neq i} q_{ij}$. The filtered probability space is $(\Omega, \mathcal{F}, (\mathcal{F}_t)_{t \geq 0}, \mathbb{P})$, with filtration generated by B_t and α_t .

381 Under \mathbb{P} , the CEA price $(P_t^A)_{t \geq 0}$ follows

382
$$dP_t^A = \mu_A(\alpha_t)P_t^A dt + \sigma_A(\alpha_t)P_t^A dB_t, \quad 0 \leq t \leq T, \quad (4.1)$$

383 with regime-specific drift $\mu_A(i)$ and volatility $\sigma_A(i) > 0$. The solution is $P_T^A =$
 384 $P_0^A \exp \left(\int_0^T \left(\mu_A(\alpha_u) - \frac{1}{2} \sigma_A^2(\alpha_u) \right) du + \int_0^T \sigma_A(\alpha_u) dB_u \right)$.

385 To price under no arbitrage, we move to a risk-neutral measure \mathbb{Q} such that $e^{-rt}P_t^A$ is a
 386 martingale. Let $\lambda_t = (\mu_A(\alpha_t) - r)/\sigma_A(\alpha_t)$ and define $\frac{d\mathbb{Q}}{d\mathbb{P}} = \exp \left(- \int_0^T \lambda_u dB_u - \frac{1}{2} \int_0^T \lambda_u^2 du \right)$.
 387 Then $\tilde{B}_t = B_t + \int_0^t \lambda_u du$ is a \mathbb{Q} -Brownian motion and

388
$$dP_t^A = rP_t^A dt + \sigma_A(\alpha_t)P_t^A d\tilde{B}_t, \quad (4.2)$$

389 or equivalently $P_T^A = P_0^A \exp \left(\int_0^T \left(r - \frac{1}{2} \sigma_A^2(\alpha_u) \right) du + \int_0^T \sigma_A(\alpha_u) d\tilde{B}_u \right)$. We keep the generator Q
 390 unchanged under \mathbb{Q} , which is standard and sufficient for pricing here.

391 To link CEA and CCER prices by regime, we introduce $\theta(i) \in [\underline{\theta}, \bar{\theta}], i = 1, \dots, m$, calibrated
 392 from CCER/CEA price ratios. When $\alpha_t = e_i$, we set

393
$$P_t^C = \theta(\alpha_t)P_t^A, \quad (4.3)$$

394 so that in regime i the CCER price is a fixed fraction $\theta(i)$ of the CEA price. Combining (4.2) and
 395 (4.3) and using Ito's formula, for fixed regime i we obtain

396
$$dP_t^C = \theta(i)dP_t^A = rP_t^C dt + \sigma_C(i)P_t^C d\tilde{B}_t, \quad \sigma_C(i) = \sigma_A(i),$$

397 so $(P_t^C)_{t \geq 0}$ also follows a regime-switching GBM under \mathbb{Q} : $dP_t^C = rP_t^C dt + \sigma_C(\alpha_t)P_t^C d\tilde{B}_t$.

398 For valuation, let $g(\cdot)$ be the marginal compliance value of one CCER at maturity T as a
 399 function of P_T^A . A simple specification with full substitutability and a floor is $g(P_T^A) =$
 400 $\max\{\nu_{\text{res}}, \theta_{\text{eff}}P_T^A\}$ with $\theta_{\text{eff}} \in [\underline{\theta}, \bar{\theta}]$. The time-zero value of a CCER unit is

401
$$V_0^C = e^{-rT} \mathbb{E}^{\mathbb{Q}}[g(P_T^A) | P_0^A = p_0^A, \alpha_0 = e_i], \quad (4.4)$$

402 where P_0^A is the current CEA price and e_i the current regime. Due to regime switches, P_T^A is not

403 lognormal and (4.4) has in general no closed form. Two standard numerical approaches are therefore
 404 used: a system of coupled PDEs, or Monte Carlo simulation (see Hu et al., 2020; Liang et al., 2022
 405 for more applications).

406 For the PDE approach, define $v_i(p, t)$ as the value at time t of one CCER when $P_t^A = p$ and
 407 $\alpha_t = e_i, i = 1, \dots, m$. Then $v = (v_1, \dots, v_m)$ solves, on $(p, t) \in (0, \infty) \times [0, T)$

$$408 \quad \frac{\partial v_i}{\partial t} + \frac{1}{2} \sigma_A^2(i) p^2 \frac{\partial^2 v_i}{\partial p^2} + rp \frac{\partial v_i}{\partial p} - rv_i + \sum_{j=1}^m q_{ij} v_j = 0, \quad (4.5)$$

409 with terminal condition $v_i(p, T) = g(p)$. Numerical schemes such as finite differences can be used
 410 to obtain $v_i(p_0^A, 0)$, so that $V_0^C = v_i(p_0^A, 0)$. For Monte Carlo, one simulates N paths of (P_t^A, α_t)
 411 under \mathbb{Q} on $[0, T]$ using (4.2) and the Markov chain with generator Q . For each path k , record
 412 $P_T^{A,(k)}$ and compute $g(P_T^{A,(k)})$; then $\hat{V}_0^C = e^{-rT} \frac{1}{N} \sum_{k=1}^N g(P_T^{A,(k)})$, which converges to V_0^C as $N \rightarrow$
 413 ∞ . Alternatively, one may simulate P_t^C directly via (4.3) and use a payoff $h(P_T^C)$, for instance
 414 $h(P_T^C) = \max\{P_T^C - K_C, v_{res}\}$ with a strike K_C , and then compute $\tilde{V}_0^C = e^{-rT} \mathbb{E}^{\mathbb{Q}}[h(P_T^C)]$. With
 415 suitable choices of g and h consistent with (4.3), the two formulations are equivalent.

416 Calibration proceeds in two steps. First, regimes are identified from exogenous
 417 variables such as daily temperature and industrial added value growth, for example by
 418 partitioning the (x, y) -plane with $y = x + c_1$ and $y = x + c_2$ and assigning each day to a
 419 regime. The transition rates q_{ij} are then estimated from empirical holding times and
 420 transition counts. Second, given regime labels, regime-specific drifts $\mu_A(i)$ and volatilities
 421 $\sigma_A(i)$ are estimated from CEA log returns, and the spread parameters $\theta(i)$ from paired
 422 CEA-CCER prices, subject to $\underline{\theta} \leq \theta(i) \leq \bar{\theta}$. Once $\{Q, \mu_A(i), \sigma_A(i), \theta(i)\}_{i=1}^m$ and r are
 423 calibrated, the regime-switching GBM fully specifies the joint dynamics of CEA and CCER

424 prices under \mathbb{Q} , and thus yields a CCER value V_θ^C that reflects regime uncertainty,
425 empirical spreads and the real options nature of CCER.

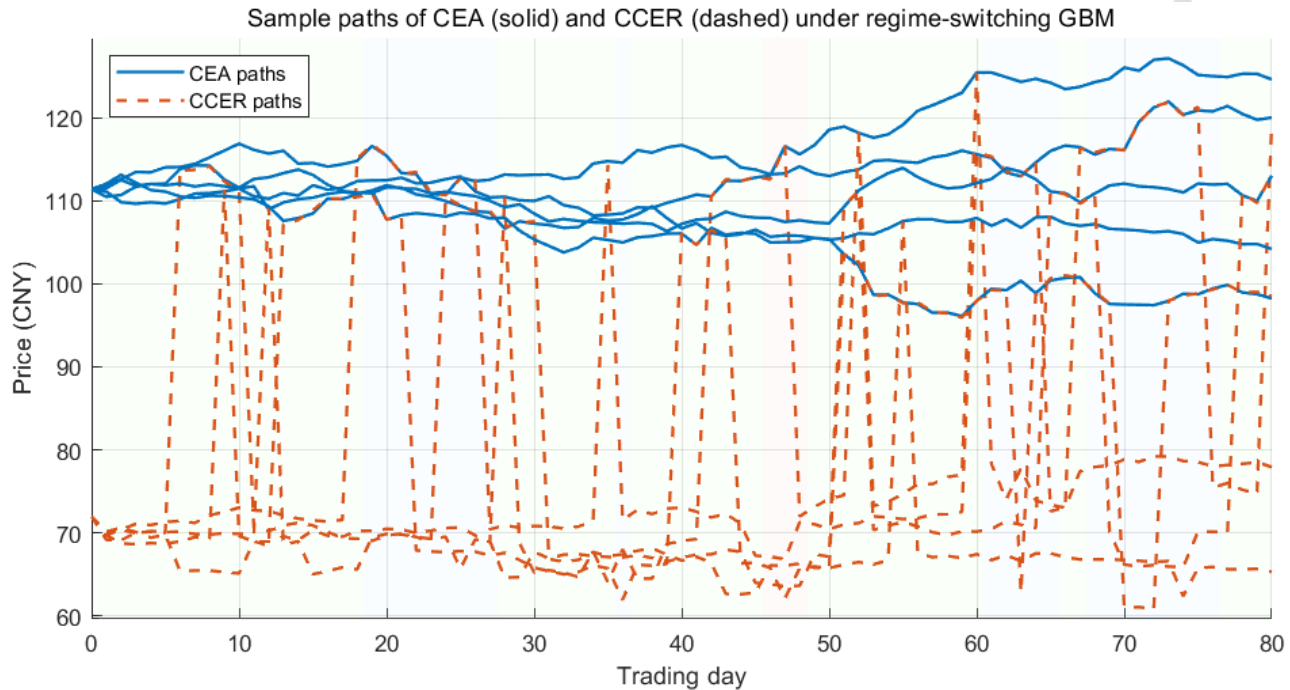
426 4.3 Numerical implementation and discussion on the results

427 This subsection uses the Matlab code (refer to Appendix C) to implement a three-regime Markov
428 switching GBM for CEA and CCER and to price a guarantee-type payoff $E[\max(CCER_T, K)]$ under
429 the risk-neutral measure. Daily 2023 CEA and CCER prices from Beijing Green Exchange are
430 combined with monthly year-on-year electricity growth. The monthly growth rates are mapped to the
431 daily grid; empirical quantiles of both electricity growth and CEA price define three regimes: regime
432 1 (low growth, low price), regime 3 (high growth, high price), and regime 2 (intermediate). If any
433 regime is too small, its days are merged into the middle regime.

434 Within each regime $s \in \{1,2,3\}$, the drift and volatility of daily CEA log returns are estimated
435 as sample mean and standard deviation, giving $\mu_A(s)$ and $\sigma_A(s)$. The Markov transition matrix P
436 is built from observed one-step regime switches. For CCER, an equilibrium relation $S_t^C \approx \theta_s S_t^A$ is
437 assumed, where θ_s is the average CCER/CEA ratio in regime s , truncated to $[0.5, 1.0]$. In simulation,
438 $S_t^C = \theta_s S_t^A$ times an idiosyncratic lognormal shock (Rasool et al., 2020; Shabbir et al., 2020; Zhang
439 et al., 2020; Hussain et al., 2021; Yan et al., 2022). The daily standard deviation of this CCER-specific
440 noise is set at $0.10\sqrt{\Delta t}$ with $Z_t \sim N(0,1)$, which generates realistic short-run deviations between
441 CCER and CEA while preserving long-run co-movement through θ_s .

442 Under the risk-neutral measure, CEA in regime s follows a GBM with drift $r - \frac{1}{2}\sigma_s^2$ and
443 volatility σ_s , with annual risk-free rate $r = 0.0435$ and time step $\Delta t = 1/252$. At each step, the
444 regime is updated using P , then CEA is evolved by the corresponding GBM, and CCER is obtained

445 as $\theta_s S_t^A$ times the idiosyncratic shock. The code simulates joint paths of CEA and CCER over
 446 $T_{trade} = 80$ trading days from end-2023 levels, with initial prices $S_0^A = 111.38$ CNY and
 447 $S_0^C = 72.00$ CNY. The initial regime is the observed last-day regime. The guarantee level is $K =$
 448 72.00 CNY.

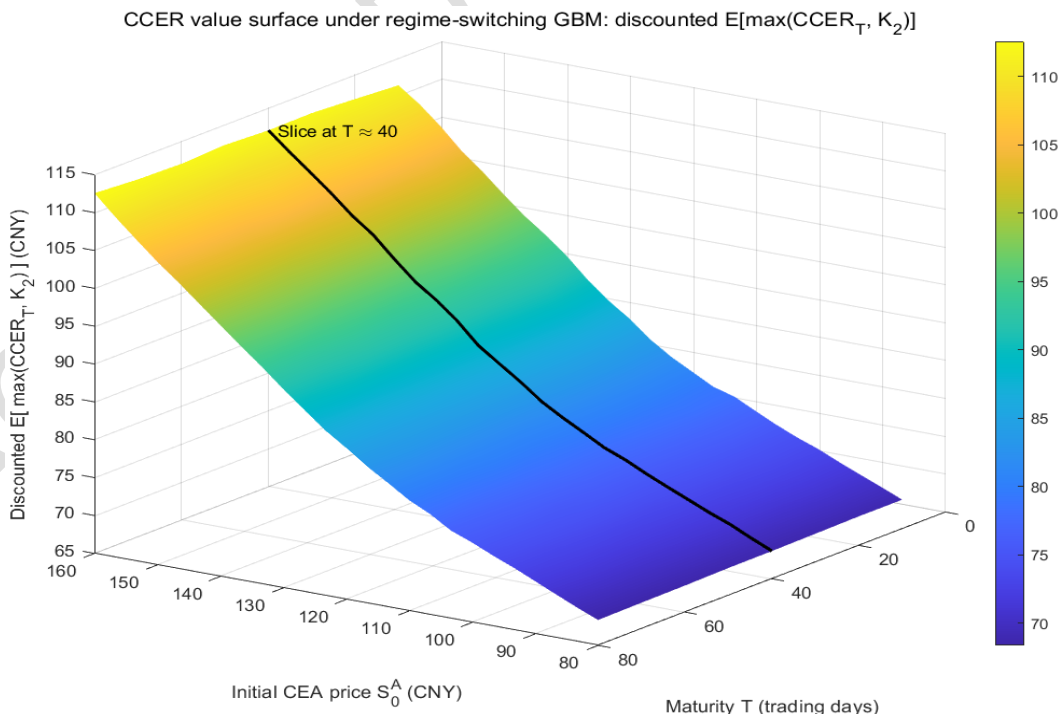


449
 450 Figure 2: Simulated CEA (solid) and CCER (dashed) price paths over 80 trading days under a three-
 451 regime switching GBM, with background color bands indicating low, medium, and high demand-
 452 price regimes

453 Figure 2 illustrates five simulated paths over 80 days. Solid lines are CEA, dashed lines CCER.
 454 The background bands show the simulated regimes: blue for regime 1, green for regime 2, red for
 455 regime 3. Regimes evolve endogenously according to P . CEA and CCER co-move at the regime
 456 scale, with higher growth of both prices and higher volatility in red bands, and flatter or downward
 457 behavior in blue bands. Regime-specific $\sigma_A(s)$ generates time-varying volatility. The larger
 458 CCER idiosyncratic noise $0.10\sqrt{\Delta t}$ produces visible but transient deviations of CCER from $\theta_s S_t^A$,
 459 consistent with CCER's lower liquidity and project heterogeneity. The paths combine long-run co-
 460 movement, regime-dependent risk and short-run spread fluctuations.

461 On this joint dynamics, the value of a single-maturity payoff $\max(CCER_T, K)$ with $T = 80$
 462 days is approximated by Monte Carlo: $PV = e^{-rT} \mathbb{E}^Q[\max(CCER_T, K)]$ with 20,000 paths. The
 463 output is $PV \approx 80.4027$ CNY per unit CCER, compared with spot $S_0^C = 72.00$ CNY and
 464 $K = 72.00$ CNY. Since $\max(CCER_T, K)$ equals one CCER plus a European call with strike K ,
 465 the excess $PV - S_0^C \approx 8.4$ CNY reflects option value from regime-driven upside and the floor at K .

466 To illustrate how the guarantee value varies with initial CEA S_0^A and maturity T , a grid is set
 467 with S_0^A from 80.00 to 160.00 CNY (25 points) and T from 10 to 80 trading days (step 10). At each
 468 grid point (S_0^A, T) , 15,000 paths of the joint process are simulated, the payoff $\max(CCER_T, K_2)$ is
 469 computed and discounted. The guarantee level is $K_2 = K_{base} + \alpha_{follow} \theta_{mid} (S_0^A - S_0^{CEA})$, where
 470 $K_{base} = 72.00$ CNY, $\theta_{mid} = 0.6257$ is the middle-regime ratio, $S_0^{CEA} = 111.38$ CNY is the current
 471 CEA price, and $\alpha_{follow} = 0.30$. Thus only 30 percent of deviations of S_0^A from S_0^{CEA} feed into the
 472 floor, which weakens the almost linear dependence that would occur under $K_2 = \theta_{mid} S_0^A$.



473
 474 Figure 3: Discounted expected value surface $E[\max(CCER_T, K_2)]$ per unit CCER under the regime-
 475 switching GBM, as a function of initial CEA price and maturity, with the guarantee level defined as
 476 a baseline plus a partially adjusting component

477 Figure 3 reports the discounted expectation $\mathbb{E}\mathbb{Q}[\max(CCER_T, K_2)]e^{-rT}$ on this grid (with
 478 simple interpolation). Along the T direction, holding S_0^A fixed, values increase with maturity because
 479 the process has more chances to enter high-demand regimes and the time value of the floor-contract
 480 outweighs discounting. Along S_0^A , each maturity slice is upward-sloping but nonlinear: with $K_2 =$
 481 $K_{base} + 0.30 \theta_{mid}(S_0^A - S_0^{CEA})$, the floor adjusts slower than the expected terminal CCER level as
 482 S_0^A rises, so the marginal impact of S_0^A gradually declines at high initial prices. In the low S_0^A
 483 region, values remain clearly above K_{base} even at short horizons, indicating a nontrivial probability
 484 of regime-driven recovery before maturity. A slice at $T \approx 40$ days(black curve) highlights this
 485 nonlinearity: near S_0^{CEA} the slope in S_0^A is steep, then flattens at higher S_0^A , confirming the damped
 486 pass-through of initial price into guarantee value under the partial-follow rule.

487 **5 Comparison and summary**

488 **5.1 Comparing micro-level and macro-level CCER valuation results**

489 This subsection compares the micro-benefit approach in Section 3 with the macro-regime
 490 switching GBM approach in Section 4. By examining the implied marginal or fair CCER price (unit:
 491 yuan/ton) of the model and aligning key calibration items (such as expected CEA settlement prices,
 492 CCER residual values, and observed CEA and CCER spot prices), the two methods are made
 493 comparable.

494 On the micro side, Section 3 studies a representative compliance enterprise minimizing expected
 495 total compliance cost under uncertain emissions, regulatory caps and residual value risk. The firm
 496 faces random annual emissions E with mean μ_E and variance σ_E^2 , allowance allocation A ,
 497 maximum CCER usage $Q_{max} = \alpha\mu_E$, expected marginal CEA settlement price \bar{p}_A , and residual

498 value v_{res} . Total cost equals upfront CCER spending plus expected CEA gap-filling cost minus
499 expected residual liquidation value. Treating $Q \in [0, Q_{max}]$ as continuous, the first-order condition
500 yields

a

marginal

willingness-to-pay

501 $p_C^*(Q) = v_{res} + (\bar{p}_A - v_{res})[1 - \Phi((A + Q - \mu_E)/\sigma_E)]$, interpreted as a weighted average of \bar{p}_A and
502 v_{res} , with the weight on \bar{p}_A given by the emission shortfall probability after purchasing Q .

503 Under the baseline calibration with offset ratio $\alpha = 0.05$, $\bar{p}_A = 115$ CNY/t, $v_{res} = 30$ CNY/t,
504 allocation $A = \mu_E$, and approximately normal emissions, the model is applied to 46 low- and normal-
505 emission firms. For each, μ_E , σ_E , Q_{max} and $p_C^*(0)$, $p_C^*(Q_{max})$, $p_C^*(Q^*)$ are computed. All firms
506 obtain $Q^* = Q_{max}$, that is optimal usage at the cap. At $Q = 0$, the shortfall probability equals 1/2 so
507 $p_C^*(0) = \frac{1}{2}(\bar{p}_A + v_{res}) = 72.50$ CNY/t. At Q_{max} the shortfall probability is much lower and the
508 marginal value drops to about 47.52 CNY/t. The emission-weighted distribution of $p_C^*(Q^*)$ is thus
509 very concentrated around 47.52 CNY/t.

510 On the macro side, Section 4 models CEA and CCER via a three-regime switching GBM
511 calibrated to 2023 Beijing data and electricity growth, with regimes capturing low, medium and high
512 demand-price environments through a finite-state Markov chain. Within each regime, CEA follows a
513 risk-neutral GBM; CCER equals a regime-dependent fraction of CEA times an idiosyncratic
514 lognormal shock with daily standard deviation $0.10\sqrt{\Delta t}$, representing CCER-specific noise. CCER is
515 then valued as a real-option-like asset whose payoff reflects its compliance substitutability and
516 residual value.

517 For a single-maturity payoff $\max(CCER_T, K)$ with $T = 80$ days, $K = 72$ CNY, $r = 0.0435$,
518 and starting prices $S_0^A = 111.38$ CNY, $S_0^C = 72.00$ CNY, Monte Carlo with 20000 paths gives $PV \approx$
519 80.40 CNY/t. The excess over spot is the value of the embedded call on CCER under regime

520 uncertainty. Extending to a grid over S_0^A and T with a guarantee K_2 anchored at 72 CNY and
 521 partially following S_0^A yields a surface $\mathbb{E}^Q[\max(CCER_T, K_2)]e^{-rT}$ that increases with T and
 522 displays nonlinear dependence on S_0^A . As follows, Table 1 summarizes representative outcomes.

523 Table 1: Comparison between micro-level and macro-level CCER valuation results

	Micro-level income approach (firm perspective)	Macro-level market approach (regime-switching GBM)
Modeling focus	Expected total compliance cost minimization for a representative firm or firm sample	Risk-neutral pricing of CCER as a real option-like asset under state-dependent price dynamics
Main uncertainty source	Firm-level emission risk (μ_E, σ_E) with prices and residual value exogenous	Stochastic CEA and CCER prices driven by a three-regime switching GBM
Decision variable or contract type	CCER purchase quantity $Q \in [0, Q_{\max}]$ chosen once per period	Holding CCER and possibly a guarantee-type contract $\max(CCER_T, K)$ or $\max(CCER_T, K_2)$
Representative price levels (CNY/t)	$p_c^*(0) = 72.50$; $p_c^*(Q_{\max}) \approx 47.52$; $p_c^*(Q^*) \approx 47.52$	$PV \approx 80.40$ at $T = 80$ days and $K = 72$; CCER spot at $t = 0: 72.00$
Treatment of residual or floor value	Constant residual value v_{res} at period end	Floor K or K_2 at maturity under regime uncertainty
Time structure	One-period static compliance decision	Multi-period stochastic evolution over up to 80 trading days

524 The micro model produces CCER values between v_{res} and \bar{p}_A , with precise levels driven by
 525 shortfall probabilities. Under the condition of homogeneous parameters and $A = \mu_E$, the marginal
 526 value converges around 47.52 CNY/t at the upper limit and is 72.50 CNY/t at zero usage, which
 527 can serve as a conservative benchmark from a static performance perspective. When applied to
 528 contracts with clear lower limits, macro models typically yield higher valuations as they price the
 529 upside potential and time value of flexibility in favorable regimes; the guaranteed rights with an

530 exercise price of $K=72$ CNY reach approximately 80.40 CNY/t, which is higher than the spot price
531 and the micro-level marginal value.

532 This difference reflects different economic roles. In the micro-scenario, CCER hedges the
533 specific emission risks of enterprises within a single compliance cycle; once the enterprise
534 comfortably meets the compliance requirements, the valuation of additional CCER approaches v_{res} .
535 In the macro-scenario, CCER is a tradable asset exposed to macro-regime shifts, with valuation using
536 the complete risk-neutral distribution of future prices, and the right-tail state is amplified due to the
537 lower bound. Therefore, earnings-based valuation is suitable for internal compliance analysis and
538 conservative reference pricing, while regime-switching GBM is more suitable for pricing structured
539 CCER products and evaluating the risk-return characteristics of CCER positions.

540 5.2 Summary and future research

541 This article constructs a comprehensive CCER valuation framework that combines the micro-
542 level income approach with the macro-level regime-switching GBM, linking compliance behavior
543 with market price dynamics.

544 At the micro level, a representative enterprise with uncertain emissions, fixed allowances and a
545 binding CCER cap chooses CCER purchase quantity Q to minimize expected total compliance cost,
546 decomposed into CCER expenditure, contingent CEA gap-filling cost and residual value of surplus
547 assets. Under a continuous emission distribution, an explicit marginal willingness-to-pay $p_c^*(Q)$ is
548 derived as a convex combination of expected CEA price and residual value, with weights given by
549 shortfall probabilities. Calibration to firm data under a baseline with $A = \mu_E$ and homogeneous
550 parameters shows optimal use at the cap and marginal values clustering near 47.52 CNY/t, with

551 $p_C^*(0) = 72.50$ CNY/t.

552 At the macro level, CEA and CCER follow a three-regime switching GBM calibrated to 2023
553 Beijing data and electricity growth. Regimes imply state-dependent drift- s and volatilities; CCER is
554 a regime-dependent fraction of CEA with idiosyncratic noise. CCER is valued as a real-option-like
555 asset. For $\max(CCER_T, K)$ with $T = 80$ days and K equal to spot, Monte Carlo yields about
556 80.40 CNY/t, above spot and micro-level marginal values. A grid over initial CEA prices and
557 maturities with K_2 defined as a baseline plus partial adjustment generates a value surface that
558 increases with T and responds nonlinearly to S_0^A , highlighting the interaction between regimes, price
559 risk and contract design.

560 The two layers achieve the following objectives together: (1) they connect firm-specific
561 emission risk and regulatory parameters to CCER valuations and optimal purchase quantities; (2)
562 they embed CCER pricing within a regime-sensitive risk-neutral framework that captures empirical
563 features including regime-dependent volatility and CEA-CCER spreads; (3) they demonstrate how
564 guarantee-type structures alter CCER value and link compliance instruments with CCER-based
565 financial products.

566 Future research could relax the micro-model assumptions on allocation, offset ratios and residual
567 values to accommodate richer heterogeneity, and expand the macro model by incorporating time-
568 varying transition intensities, jump processes or stochastic volatility, alongside a more granular CEA-
569 CCER spread process. A particularly promising direction involves tighter coupling of the two layers,
570 where macro price dynamics generate endogenous inputs for the micro model while firm-level CCER
571 demand feeds back into the market model, thereby enabling analysis of the feedback mechanisms
572 among compliance behavior, policy design and price formation in support of carbon peaking and

573 neutrality objectives.

574 References

575 [1]Adade, S.Y.S.S., Lin, H., Johnson, N.A.N., et al. Advanced food contaminant detection through
576 multi-source data fusion: Strategies, applications, and future perspectives[J]. Trends in Food
577 Science & Technology, 2025, 156.

578 [2]Alessi, L., Ossola, E., Panzica, R. When do investors go green? Evidence from a time-varying
579 asset-pricing model[J]. International Review of Financial Analysis, 2023, 90: 102898.

580 [3]Barker, R., Lennard, A., Penman, S., et al. Accounting for intangible assets: suggested
581 solutions[J]. Accounting and Business Research, 2022, 52(6): 601-630.

582 [4]Bolton, P., Kacperczyk, M. Are carbon emissions associated with stock returns? Comment[J].
583 Review of Finance, 2024, 28(1): 107-109.

584 [5]Chen, M., Lai, E. Carbon Asset Management System and Trading Strategies: Empowering Listed
585 Companies in Value Reassessment and Sustainable Development[J]. Advances in Management and
586 Intelligent Technologies, 2025, 1(6).

587 [6]Chevallier, J., Goutte, S., Ji, Q., et al. Green finance and the restructuring of the oil-gas-coal
588 business model under carbon asset stranding constraints[J]. Energy Policy, 2021, 149: 112055.

589 [7]Dong, X., Yoon, S.M. Effect of weather and environmental attentions on financial system risks:
590 Evidence from Chinese high- and low-carbon assets[J]. Energy Economics, 2023, 121: 106680.

591 [8]Dutta, A., Dutta, P. Geopolitical risk and renewable energy asset prices: Implications for
592 sustainable development[J]. Renewable Energy, 2022, 196: 518-525.

593 [9]Green, J.F. Does carbon pricing reduce emissions? A review of ex-post analyses[J].
594 Environmental Research Letters, 2021, 16(4): 043004.

595 [10]Hao, J., Deng, Z., Li, J., et al. How to price a dataset: a deep learning framework for data
596 monetization with alternative data[J]. Humanities and Social Sciences Communications, 2025, 12:
597 1736.

598 [11]Hu, D., Sun, T., Yao, L., et al. Monte Carlo: A flexible and accurate technique for modeling
599 light transport in food and agricultural products[J]. Trends in Food Science & Technology, 2020,
600 102: 280-290.

601 [12]Hussain, S., Hussain, S., Aslam, Z., et al. Impact of Different Water Management Regimes on
602 the Growth, Productivity, and Resource Use Efficiency of Dry Direct Seeded Rice in Central
603 Punjab-Pakistan[J]. Agronomy-Basel, 2021, 11(6).

604 [13]Jeny, A., Moldovan, R. Accounting for intangible assets - insights from meta-analysis of R&D
605 research[J]. *Journal of Accounting Literature*, 2022, 44(1): 40-71.

606 [14]Langley, P., Bridge, G., Bulkeley, H., et al. Decarbonizing capital: Investment, divestment and
607 the qualification of carbon assets[J]. *Economy and Society*, 2021, 50(3): 494-516.

608 [15]Li, W., Zhang, C., Ma, T., et al. Estimation of summer maize biomass based on a crop growth
609 model[J]. *Emirates Journal Of Food And Agriculture*, 2021, 33(9): 742-750.

610 [16]Liang, Z., Li, J., Liang, J., et al. Investigation into Experimental and DEM Simulation of Guide
611 Blade Optimum Arrangement in Multi-Rotor Combine Harvesters[J]. *Agriculture-Basel*, 2022,
612 12(3).

613 [17]Liu, Y., Tian, L., Sun, H., et al. Option pricing of carbon asset and its application in digital
614 decision-making of carbon asset[J]. *Applied Energy*, 2022, 310: 118375.

615 [18]Liu, Y., Tian, L., Xie, Z., et al. Option to survive or surrender: Carbon asset management and
616 optimization in thermal power enterprises from China[J]. *Journal of Cleaner Production*, 2021, 314:
617 128006.

618 [19]Liu, Y., Lu, X., Sun, H.P., et al. Optimization of carbon performance evaluation and its
619 application to strategy decision for investment of green technology innovation[J]. *Journal of
620 Environmental Management*, 2023, 325A: 116593.

621 [20]Liu, Y., Sun, H.P., Meng, B., et al. How to purchase carbon emission right optimally for energy-
622 consuming enterprises? Analysis based on optimal stopping model[J]. *Energy Economics*, 2023,
623 124: 106758.

624 [21]Mahmood, F., Ali, M., Khan, M., et al. A review of biochar production and its employment in
625 synthesizing carbon-based materials for supercapacitors[J]. *Industrial Crops and Products*, 2025,
626 227.

627 [22]Mengesha, I., Roy, D. Carbon pricing drives critical transition to green growth[J]. *Nature
628 Communications*, 2025, 16: 1321.

629 [23]Nazir, M.J., Li, G., Nazir, M.M., et al. Harnessing soil carbon sequestration to address climate
630 change challenges in agriculture[J]. *Soil & Tillage Research*, 2023, 237.

631 [24]Ni, J., Xue, Y., Zhou, Y., et al. Rapid identification of greenhouse tomato senescent leaves based
632 on the sucrose-spectral quantitative prediction model[J]. *Biosystems Engineering*, 2024, 238: 200-
633 211.

634 [25]Ni, J., Xue, Y., Zhou, Y., et al. Rapid identification of greenhouse tomato senescent leaves based
635 on the sucrose-spectral quantitative prediction model[J]. *Biosystems Engineering*, 2024, 238: 200-
636 211.

637 [26]Pechlivanidis, E., Ginoglou, D., Barmpoutis, P. Can intangible assets predict future
638 performance? A deep learning approach[J]. International Journal of Accounting & Information
639 Management, 2022, 30(1): 61-72.

640 [27]Rasool, G., Guo, X., Wang, Z., et al. Coupling fertigation and buried straw layer improves
641 fertilizer use efficiency, fruit yield, and quality of greenhouse tomato[J]. Agricultural Water
642 Management, 2020, 239.

643 [28]Raza, S., Irshad, A., Margenot, A., et al. Inorganic carbon is overlooked in global soil carbon
644 research: A bibliometric analysis[J]. Geoderma, 2024, 443.

645 [29]Sadalage, P.S., Dar, M.A., Bhor, R.D., et al. Optimization of biogenic synthesis of
646 biocompatible platinum nanoparticles with catalytic, enzyme mimetic and antioxidant activities[J].
647 Food Bioscience, 2022, 50.

648 [30]Shabbir, A., Mao, H., Ullah, I., et al. Effects of Drip Irrigation Emitter Density with Various
649 Irrigation Levels on Physiological Parameters, Root, Yield, and Quality of Cherry Tomato[J].
650 Agronomy-Basel, 2020, 10(11).

651 [31]Shao, L., Gong, J., Fan, W., et al. Cost Comparison between Digital Management and
652 Traditional Management of Cotton Fields-Evidence from Cotton Fields in Xinjiang, China[J].
653 Agriculture-Basel, 2022, 12(8).

654 [32]Siddique, M.A., Nobanee, H., Hasan, M.B., et al. How do energy markets react to climate
655 policy uncertainty? Fossil vs. renewable and low-carbon energy assets[J]. Energy Economics, 2023,
656 128: 107195.

657 [33]Su, C.W., Pang, L.D., Qin, M., et al. The spillover effects among fossil fuel, renewables and
658 carbon markets: Evidence under the dual dilemma of climate change and energy crises[J]. Energy,
659 2023, 274: 127304.

660 [34]Van Benthem, A.A., Crooks, E., Giglio, S., et al. The effect of climate risks on the interactions
661 between financial markets and energy companies[J]. Nature Energy, 2022, 7: 690-697.

662 [35]Van Criekingen, K., Bloch, C., Eklund, C. Measuring intangible assets - A review of the state of
663 the art[J]. Journal of Economic Surveys, 2022, 36(5): 1539-1558.

664 [36]Van den Bremer, T.S., Van der Ploeg, F. The risk-adjusted carbon price[J]. American Economic
665 Review, 2021, 111(9): 2782-2810.

666 [37]von Dulong, A. Concentration of asset owners exposed to power sector stranded assets may
667 trigger climate policy resistance[J]. Nature Communications, 2023, 14: 6442.

668 [38]Wang, H., Liu, J., Zhang, L. Carbon emissions and assets pricing - evidence from Chinese listed
669 firms[J]. China Journal of Economics, 2022, 9(2): 28-75.

670 [39]Wang, H., Kang, Z., Yu, S., et al. Feasibility analysis of developing methane reduction
 671 methodologies in the oil and gas sector under the ccer reboot context[J]. Energy Storage Science
 672 and Technology, 2025, 14(4): 1709.

673 [40]Wang, X., Li, J., Ren, X. Asymmetric causality of economic policy uncertainty and oil volatility
 674 index on time-varying nexus of the clean energy, carbon and green bond[J]. International Review of
 675 Financial Analysis, 2022, 83: 102306.

676 [41]Xu, H., Yin, H., Liu, Y., et al. Regional Winter Wheat Yield Prediction and Variable Importance
 677 Analysis Based on Multisource Environmental Data[J]. Agronomy-Basel, 2024, 14(8).

678 [42]Xu, H., Yin, H., Liu, Y., et al. Regional Winter Wheat Yield Prediction and Variable Importance
 679 Analysis Based on Multisource Environmental Data[J]. Agronomy-Basel, 2024, 14(8).

680 [43]Yan, H., Ma, J., Zhang, J., et al. Effects of film mulching on the physiological and
 681 morphological parameters and yield of cucumber under insufficient drip irrigation[J]. Irrigation And
 682 Drainage, 2022, 71(4): 897-911.

683 [44]Yang, P., Yang, L. Asset pricing and nominal price illusion in China[J]. Humanities and Social
 684 Sciences Communications, 2022, 9: 118.

685 [45]Zhang, C., Li, X., Yan, H., et al. Effects of irrigation quantity and biochar on soil physical
 686 properties, growth characteristics, yield and quality of greenhouse tomato[J]. Agricultural Water
 687 Management, 2020, 241.

688 [46]Zhang, J. Corporate carbon emissions and market value[J]. Scientific Reports, 2025, 15: 30593.

689 [47]Zhang, L., Song, X., Niu, Y., et al. Estimating Winter Wheat Plant Nitrogen Content by
 690 Combining Spectral and Texture Features Based on a Low-Cost UAV RGB System throughout the
 691 Growing Season[J]. Agriculture-Basel, 2024, 14(3).

692 [48]Zhang, S., Xue, X., Chen, C., et al. Development of a low-cost quadrotor UAV based on ADRC
 693 for agricultural remote sensing[J]. International Journal Of Agricultural And Biological
 694 Engineering, 2019, 12(4): 82-87.

695 [49]Zhang, Z., Li, J., Guan, D. Value chain carbon footprints of Chinese listed companies[J]. Nature
 696 Communications, 2023, 14: 2794.

697

698 **Appendix A**

699 Table 2 Annual carbon emission data for low-emission enterprises (tons)

Ticker symbol	m_{i1}	m_{i2}	m_{i3}	Ticker symbol	m_{i1}	m_{i2}	m_{i3}
603388	5969	5427	4884	603778	5469	4972	4475

002431	14559	13236	11912	300008	27852	25320	22788
300536	20967	19061	17155	600072	26117	23743	21368
000037	7867	7152	6437	603717	20927	19025	17122
000993	8405	7641	6876	000711	18504	16822	15140

Source: CSMAR Database

Table 3 Annual carbon emission data for normal-emission enterprises (tons)

Ticker symbol	m_{j1}	m_{j2}	m_{j3}	Ticker symbol	m_{j1}	m_{j2}	m_{j3}	Ticker symbol	m_{j1}	m_{j2}	m_{j3}
600011	9076451	8251319	7426187	600025	839682	763347	687012	603828	109891	99901	89911
600795	3927170	3570155	3213139	000959	6749599	6135999	5522399	002542	530198	481998	433799
601991	5552259	5047508	4542757	000761	4723905	4294459	3865013	002564	716273	651157	586042
600027	6756622	6142383	5528145	600126	1990390	1809445	1628501	002628	138814	126195	113575
600023	3795945	3450859	3105773	000778	196041	178219	160397	002663	68298	62089	55880
000539	2368211	2152919	1937627	600307	1431482	1301347	1171213	002761	10519590	9563263	8606937
600021	1540961	1400873	1260786	600782	4447745	4043405	3639064	002775	72117	65561	59005
000027	2276119	2069199	1862279	000709	3706154	3369231	3032308	002140	498744	453404	408063
002608	2132345	1938495	1744646	600569	2818325	2562113	2305902	300055	65169	59245	53320
600578	1708917	1553561	1398205	600282	4746223	4314748	3883274	300237	52063	47330	42597
600575	1445654	1314231	1182808	601005	1693446	1539496	1385546	300517	95146	86496	77847
600157	1533348	1393952	1254557	000825	3723184	3384713	3046241	000862	62357	56688	51019
000543	1126340	1023946	921551	600117	557233	506575	455918	300649	104958	95417	85875
600642	2127118	1933743	1740369	000717	2052221	1865655	1679090	300712	95242	86584	77925
600863	584866	531697	478527	600019	21523775	19567068	17610361	600039	7472533	6793212	6113891
000600	534253	485685	437116	000932	5453736	4957942	4462148	002116	500880	455345	409811
000767	1034726	940660	846594	600507	1269384	1153986	1038587	600133	799036	726396	653757
000966	723281	657528	591775	000898	5667263	5152057	4636852	600170	14171007	12882733	11594460
001896	782009	710918	639826	600010	3162971	2875428	2587885	600248	15423990	14021809	12619628
600780	425868	387153	348437	600022	4586444	4169495	3752545	600284	1135404	1032186	928967
600509	583520	530472	477425	600231	1027681	934255	840830	600463	61704	56094	50485
000690	452755	411595	370436	601003	4383901	3985365	3586828	600491	114836	104396	93956
600744	691180	628346	565511	600808	3801689	3456081	3110473	600502	5764712	5240647	4716582
000899	170012	154556	139101	600295	1641085	1491896	1342706	600512	526711	478828	430946
000531	238187	216534	194881	000655	137061	124601	112141	600606	29341384	26673985	24006587
600396	249379	226708	204037	600581	1509440	1372218	1234997	600667	1620650	1473318	1325987
002893	82005	74550	67095	000629	484185	440168	396152	600820	6238700	5671545	5104391
600969	204230	185664	167098	603878	161881	147165	132448	600846	431993	392721	353449
000791	95916	87197	78477	000923	190663	173330	155997	600853	753134	684667	616201
000601	317822	288929	260036	000708	8055406	7323096	6590786	600970	2317066	2106424	1895782
600483	885339	804853	724368	601969	47961	43601	39241	601117	7972458	7247689	6522920
000883	1542108	1401917	1261725	002110	4542493	4129539	3716585	601186	70552790	64138900	57725010
600900	1554752	1413411	1272070	002075	355375	323068	290761	601390	37510749	34100681	30690613
601985	3887484	3534076	3180668	600477	483255	439323	395391	601611	3506691	3187901	2869111
600886	1218380	1107618	996856	600496	1036042	941856	847670	601618	33385953	30350867	27315780
601669	26125183	23750167	21375150	601968	462657	420597	378537	601668	122315835	111196213	100076592

600821	158991	144538	130084	002756	377439	343127	308814	601669	26125183	23750167	21375150
600452	97359	88508	79657	200761	3740889	3400808	3060727	601789	945971	859974	773977
600995	124867	113515	102164	900936	1575137	1431943	1288748	601800	29555593	26868721	24181849
600116	1005080	913709	822338	002132	64877	58979	53081	603316	101724	92477	83229
600505	37156	33779	30401	002135	328280	298436	268593	603637	102229	92935	83642
000692	192555	175050	157545	002318	280555	255050	229545	603098	233934	212667	191400
600644	149033	135484	121936	002443	287503	261366	235229	603843	680770	618882	556994
000040	108142	98311	88480	002478	162868	148062	133255	603955	46973	42703	38432
000537	299017	271833	244650	002541	1520498	1382271	1244044	603959	92167	83788	75409
600167	98361	89419	80477	000629	484185	440168	396152	000032	1708014	1552740	1397466
600982	712794	647995	583195	000708	3270983	2973621	2676259	603929	101247	92043	82838
600236	274713	249739	224765	000709	3706154	3369231	3032308	002047	166202	151093	135983
600101	84140	76490	68841	000717	2052221	1865655	1679090	002081	449608	408735	367861
002039	36605	33277	29949	000961	9579035	8708214	7837393	002163	196604	178730	160857
600163	183816	167106	150395	600022	4586444	4169495	3752545	002325	149391	135810	122229
600674	50586	45988	41389	600894	433825	394386	354948	002375	585633	532393	479154
601619	60570	55064	49557	002743	318579	289617	260656	002482	56893	51721	46549
000875	755307	686642	617978	000928	1605125	1459205	1313284	002620	129069	117335	105602
002479	524052	476411	428770	000628	691222	628383	565545	002713	285503	259548	233594
600098	2634239	2394763	2155286	600939	3477904	3161731	2845558	002789	101022	91838	82654
002256	681601	619637	557673	000010	247465	224968	202471	002811	86688	78807	70926
002015	1129772	1027065	924359	000065	1761791	1601628	1441466	002822	645172	586520	527868
601016	232664	211513	190362	000090	2343598	2130543	1917489	002830	83769	76153	68538
600149	36910	33555	30199	000498	5430569	4936881	4443193	002856	71940	65400	58860
000722	31110	28282	25454	002307	997813	907102	816392	300117	70924	64476	58028
000591	303997	276361	248725	002051	113708	103371	93034	300621	755394	686722	618050
300335	63694	57904	52114	002060	949279	862981	776683	600193	94218	85652	77087
000155	231426	210387	189348	002061	3041286	2764805	2488325	601886	1443949	1312681	1181413
600979	85830	78027	70224	002062	940424	854931	769438	603030	131737	119761	107785

Source: CSMAR Database

702

703

Appendix B

```

704 %=====
705 % Income-Approach CCER Valuation (LaTeX-based, Word-data only)
706 %=====
707 clear;clc;close all;
708
709 %% 1. Global parameters
710
711 alpha = 0.05; % Max CCER offset ratio
712 pA_bar = 115; % Expected marginal CEA settlement price (CNY/t)
713 v_res = 30; % Residual value of CCER (CNY/t), must be < pA_bar
714
715 % Historical daily prices from Word data (for reference only, not used later)
716 aprice = [ ...
717     138.00 110.40 90.00 72.00 59.00 51.47 61.80 74.20 74.20 ...
718     89.00 74.00 106.80 86.00 102.00 115.64 138.50 111.00 92.22 73.80 75.00 ...
719     88.77 106.60 125.00 149.64 144.30 131.75 134.00 124.00 100.90 121.00 ...
720     130.12 139.00 127.00 127.00 121.77 142.00 121.88 127.00 120.00 130.00 ...
721     127.00 130.00 132.53 122.50 133.50 128.00 128.00 123.03 124.00 127.50 ...
722     119.18 123.57 123.77 121.28 123.00 130.29 121.35 115.13 125.25 124.94 ...
723     124.17 127.93 125.17 121.38 117.72 126.25 123.03 116.89 105.28 120.71 ...
724     118.88 118.44 121.37 124.41 113.92 119.90 115.90 119.96 113.01 109.92 ...
725     118.49 109.91 108.16 121.72 116.00 103.32 100.00 110.00 109.00 110.00 ...
726     114.34 95.00 85.06 102.00 107.00 115.00 116.00 112.00 111.38];
727
728 cprice = [ ...

```

```

729 95.00 95.00 95.00 109.00 88.00 80.00 90.00 90.89 47.00 78.00 ...
730 80.00 80.00 56.40 90.00 80.00 82.00 80.00 80.00 80.34 80.00 75.00 ...
731 80.00 80.00 86.96 80.00 80.01 84.81 88.00 65.64 80.00 69.70 81.40 80.00 ...
732 69.38 70.50 80.44 83.90 78.23 86.00 86.99 80.00 80.00 74.77 77.63 74.50 ...
733 75.00 80.10 85.40 80.00 74.00 70.42 78.00 79.51 79.14 85.00 80.00 75.00 ...
734 65.00 65.00 74.60 65.01 70.00 90.00 70.00 72.00 72.00 72.00 72.00];
735
736 %% 2. Firm-level emission data from Word (appendix tables)
737
738 % 2.1 Low-emission firms (Table 2)
739 % Columns: [Ticker, E_upper, E_mid, E_lower]
740 low_tab = [ ...
741 603388 5969 5427 4884; ...
742 2431 14559 13236 11912; ... % keep numeric consistency for leading zero tickers
743 300536 20967 19061 17155; ...
744 37 7867 7152 6437; ...
745 993 8405 7641 6876; ...
746 603778 5469 4972 4475; ...
747 300008 27852 25320 22788; ...
748 600072 26117 23743 21368; ...
749 603717 20927 19025 17122; ...
750 711 18504 16822 15140];
751
752 ticker_low = low_tab(:,1);
753 E_up_low = low_tab(:,2);
754 E_mid_low = low_tab(:,3);
755 E_lo_low = low_tab(:,4);
756
757 zband = 1.64; % ~90% CI
758 muE_low = E_mid_low; % mean emissions
759 sigmaE_low = (E_up_low - E_lo_low) / (2*zband);
760 sigmaE_low(sigmaE_low <= 0) = 1e-6;
761
762 A_low = muE_low; % allowance = mean emissions
763 Qmax_low = alpha * muE_low; % max CCER usage
764
765 % 2.2 Normal-emission firms (Table 3)
766 % Columns: [Ticker, E_upper, E_mid, E_lower]
767 norm_tab = [ ...
768 600011 9076451 8251319 7426187; ...
769 600795 3927170 3570155 3213139; ...
770 601991 5552259 5047508 4542757; ...
771 600027 6756622 6142383 5528145; ...
772 600023 3795945 3450859 3105773; ...
773 539 2368211 2152919 1937627; ...
774 600021 1540961 1400873 1260786; ...
775 27 2276119 2069199 1862279; ...
776 2608 2132345 1938495 1744646; ...
777 600578 1708917 1553561 1398205; ...
778 600575 1445654 1314231 1182808; ...
779 600157 1533348 1393952 1254557; ...
780 543 1126340 1023946 921551; ...
781 600642 2127118 1933743 1740369; ...
782 600863 584866 531697 478527; ...
783 600 534253 485685 437116; ...
784 767 1034726 940660 846594; ...
785 966 723281 657528 591775; ...
786 1896 782009 710918 639826; ...
787 600780 425868 387153 348437; ...
788 600509 583520 530472 477425; ...
789 690 452755 411595 370436; ...
790 600744 691180 628346 565511; ...
791 899 170012 154556 139101; ...
792 531 238187 216534 194881; ...
793 600396 249379 226708 204037; ...
794 2893 82005 74550 67095; ...
795 600969 204230 185664 167098; ...
796 791 95916 87197 78477; ...
797 601 317822 288929 260036; ...
798 600483 885339 804853 724368; ...
799 883 1542108 1401917 1261725; ...
800 600900 1554752 1413411 1272070; ...
801 601985 3887484 3534076 3180668; ...
802 600886 1218380 1107618 996856; ...
803 601669 26125183 23750167 21375150];
804
805 ticker_norm = norm_tab(:,1);
806 E_up_norm = norm_tab(:,2);
807 E_mid_norm = norm_tab(:,3);
808 E_lo_norm = norm_tab(:,4);
809
810 muE_norm = E_mid_norm;
811 sigmaE_norm = (E_up_norm - E_lo_norm) / (2*zband);
812 sigmaE_norm(sigmaE_norm <= 0) = 1e-6;
813
814 A_norm = muE_norm;
815 Qmax_norm = alpha * muE_norm;
816
817 %% 3. CCER marginal willingness-to-pay function (LaTeX-based)
818

```

```

819 pc_fun = @(Q, muE, sigmaE, A) ...
820     v_res + (pA_bar - v_res).* (1 - normedf( (A + Q - muE) ./ sigmaE ));
821
822 phi = @(x) exp(-0.5*x.^2) ./ sqrt(2*pi);
823
824 %% 4. Merge samples and compute firm-level results
825
826 ticker_all = [ticker_low; ticker_norm];
827 muE_all = [muE_low; muE_norm];
828 sigma_all = [sigmaE_low; sigmaE_norm];
829 A_all = [A_low; A_norm];
830 Qmax_all = [Qmax_low; Qmax_norm];
831
832 Nfirm = numel(ticker_all);
833 Qstar_all = zeros(Nfirm,1);
834 pC_Q0_all = zeros(Nfirm,1);
835 pC_Qmax_all = zeros(Nfirm,1);
836 pC_Qstar_all = zeros(Nfirm,1);
837
838 % Representative firm: median mu_E
839 [~,idx_med] = min(abs(muE_all - median(muE_all)));
840 idx_rep = idx_med;
841
842 nQgrid = 50;
843 Qgrid_rep = linspace(0, Qmax_all(idx_rep), nQgrid);
844 pe_rep = pc_fun(Qgrid_rep, muE_all(idx_rep), sigma_all(idx_rep), A_all(idx_rep));
845
846 fprintf('===== CCER Valuation (Firm-Level) =====\n');
847 fprintf('Global parameters:\n');
848 fprintf(' alpha = %.4f (max CCER offset ratio)\n', alpha);
849 fprintf(' pA_bar = %.2f CNY/t (expected marginal CEA settlement price)\n', pA_bar);
850 fprintf(' v_res = %.2f CNY/t (residual value of CCER)\n\n', v_res);
851
852 fprintf('Firm-level parameters and key prices:\n');
853 fprintf('%-10s %-14s %-14s %-14s %-14s %-14s\n', ...
854     'Ticker','mu_E','sigma_E','Qmax','pC(Q=0)','pC(Qmax)','pC(Q*)');
855
856 for i = 1:Nfirm
857     muE_i = muE_all(i);
858     sig_i = sigma_all(i);
859     A_i = A_all(i);
860     Qmax_i = Qmax_all(i);
861
862     % Marginal prices at Q=0 and Q=Qmax
863     pC_Q0_all(i) = pc_fun(0, muE_i, sig_i, A_i);
864     pC_Qmax_all(i) = pc_fun(Qmax_i, muE_i, sig_i, A_i);
865
866     % Optimal Q* by minimizing expected total cost
867     obj = @(q) ETC_single(q, muE_i, sig_i, A_i, pA_bar, v_res, phi, @normedf);
868     [Qstar_i, ~] = fminbnd(obj, 0, Qmax_i);
869
870     Qstar_all(i) = Qstar_i;
871     pC_Qstar_all(i) = pc_fun(Qstar_i, muE_i, sig_i, A_i);
872
873     fprintf('%-10d %-14.2f %-14.2f %-14.2f %-14.2f %-14.2f\n', ...
874         ticker_all(i), muE_i, sig_i, Qmax_i, ...
875         pC_Q0_all(i), pC_Qmax_all(i), pC_Qstar_all(i));
876 end
877
878 %% 5. Weighted average theoretical CCER prices (mu_E weights)
879
880 weight = muE_all / sum(muE_all);
881 avg_pC_Q0 = sum(weight .* pC_Q0_all);
882 avg_pC_Qmax = sum(weight .* pC_Qmax_all);
883 avg_pC_Qstar = sum(weight .* pC_Qstar_all);
884
885 fprintf('\nWeighted-average theoretical CCER prices (weights = mu_E):\n');
886 fprintf(' Mean p_C^(Q=0) = %.2f CNY/t\n', avg_pC_Q0);
887 fprintf(' Mean p_C^(Q=Qmax) = %.2f CNY/t\n', avg_pC_Qmax);
888 fprintf(' Mean p_C^(Q=Q*) = %.2f CNY/t\n', avg_pC_Qstar);
889
890 %% 6. Explicit description of Figure 1 (representative firm)
891
892 rep_ticker = ticker_all(idx_rep);
893 rep_muE = muE_all(idx_rep);
894 rep_sigmaE = sigma_all(idx_rep);
895 rep_A = A_all(idx_rep);
896 rep_Qmax = Qmax_all(idx_rep);
897 rep_Q0 = 0;
898 rep_Qstar = Qstar_all(idx_rep);
899 rep_pC_Q0 = pC_Q0_all(idx_rep);
900 rep_pC_Qmax = pC_Qmax_all(idx_rep);
901 rep_pC_Qstar = pC_Qstar_all(idx_rep);
902
903 fprintf('Figure 1 (Representative firm p_C^(Q) curve):\n');
904 fprintf(' Representative firm ticker : %d\n', rep_ticker);
905 fprintf(' Representative firm mu_E : %.2f t CO2\n', rep_muE);
906 fprintf(' Representative firm sigma_E : %.2f t CO2\n', rep_sigmaE);
907 fprintf(' Representative firm allowance A : %.2f t CO2\n', rep_A);
908 fprintf(' Representative firm Qmax : %.2f t CO2\n', rep_Qmax);

```

```

909 fprintf(' Horizontal axis: Q in million t CO2 from %.2f to %.2f\n', ...
910     rep_Q0/1e6, rep_Qmax/1e6);
911 fprintf(' Vertical axis: p_C^(Q) in CNY/t\n');
912 fprintf(' Curve: p_C^(Q) for Q in [0, Qmax]\n');
913 fprintf(' Horizontal reference line: p_A_bar = %.2f CNY/t\n', pA_bar);
914 fprintf(' Horizontal reference line: v_res = %.2f CNY/t\n', v_res);
915 fprintf(' Marked point at Q=0 : Q = %.2f, p_C^(0) = %.2f CNY/t\n', ...
916     rep_Q0, rep_pC_Q0);
917 fprintf(' Marked point at Q=Qmax : Q = %.2f, p_C^(Qmax) = %.2f CNY/t\n', ...
918     rep_Qmax, rep_pC_Qmax);
919 fprintf(' Marked point at Q=Q* : Q* = %.2f, p_C^(Q*) = %.2f CNY/t\n', ...
920     rep_Qstar, rep_pC_Qstar);
921
922 %% 7. Explicit description of Figure 2 (distribution of p_C^(Q*))
923
924 pC_min = min(pC_Qstar_all);
925 pC_max = max(pC_Qstar_all);
926 pC_mean = mean(pC_Qstar_all);
927 pC_median = median(pC_Qstar_all);
928 pC_std = std(pC_Qstar_all);
929
930 fprintf('Figure 2 (Distribution of firm-level optimal marginal CCER prices p_C^(Q*)):\n');
931 fprintf(' Sample size (number of firms) : %d\n', Nfirm);
932 fprintf(' Horizontal axis: p_C^(Q*) in CNY/t\n');
933 fprintf(' Vertical axis: number of firms (histogram counts)\n');
934 fprintf(' Range of p_C^(Q*) : [%2.2f, %2.2f] CNY/t\n', pC_min, pC_max);
935 fprintf(' Mean of p_C^(Q*) : %.2f CNY/t\n', pC_mean);
936 fprintf(' Median of p_C^(Q*) : %.2f CNY/t\n', pC_median);
937 fprintf(' Std. deviation of p_C^(Q*) : %.2f CNY/t\n', pC_std);
938
939 %% 8. Figures (two figures only)
940
941 % Figure 1: Representative firm p_C^(Q) curve
942 figure;
943 plot(Qgrid_rep/1e6, pc_rep, 'b-', 'LineWidth', 2); hold on;
944 yline(pA_bar,'r-','LineWidth',1.5);
945 yline(v_res,'k-','LineWidth',1.5);
946 xlabel('Q (million t CO2)');
947 ylabel('p_C^(Q) (CNY/t)');
948 title(sprintf('Representative Firm (Ticker=%d): p_C^(Q)', rep_ticker));
949 legend('p_C^(Q)', 'p_A^{bar}', 'v_{res}', 'Location','best');
950 grid on;
951
952 plot(rep_Q0/1e6, rep_pC_Q0,'ko','MarkerFaceColor','k');
953 text(rep_Q0/1e6, rep_pC_Q0, ' Q=0','VerticalAlignment','bottom');
954
955 plot(rep_Qmax/1e6, rep_pC_Qmax, 'ko','MarkerFaceColor','k');
956 text(rep_Qmax/1e6, rep_pC_Qmax, ' Q=Q_{max}','VerticalAlignment','top');
957
958 plot(rep_Qstar/1e6, rep_pC_Qstar, 'ro','MarkerFaceColor','r');
959 text(rep_Qstar/1e6, rep_pC_Qstar, ' Q=Q^{*}','VerticalAlignment','bottom');
960
961 %% Figure 2: Distribution of optimal marginal CCER prices p_C^(Q*)
962 figure;
963 histogram(pC_Qstar_all, 'FaceColor',[0.2 0.6 0.8]);
964 xlabel('p_C^(Q^{*}) (CNY/t)');
965 ylabel('Number of firms');
966 title('Distribution of Firm-Level Optimal CCER Marginal Prices');
967 grid on;
968
969 %% 9. Auxiliary function: expected total cost for a single firm
970
971 function ETC = ETC_single(Q, muE, sigmaE, A, pA_bar, v_res, phi, normcdf_handle)
972     T = A + Q;
973     a = (T - muE) ./ sigmaE;
974     Phi_a = normcdf_handle(a);
975     phi_a = phi(a);
976
977     E_gap_pos = sigmaE .* (phi_a - a .* (1 - Phi_a)); % E[(E - T)_+]
978     E_surplus_pos = sigmaE .* (phi_a + a .* Phi_a); % E[(T - E)_+]
979
980     pC_star = v_res + (pA_bar - v_res) .* (1 - Phi_a);
981
982     ETC = pC_star .* Q + pA_bar .* E_gap_pos - v_res .* E_surplus_pos;
983 end
984

```

985 Appendix C

```

986 function main_regime_switching_CCER_smooth_v2
987 clc; clear; close all;
988
989 CEA_2023 = [ ...
990 138.00 110.40 90.00 59.00 51.47 61.80 74.20 74.20 74.20 ...
991 89.00 74.00 106.80 86.00 102.00 115.64 138.50 111.00 92.22 73.80 75.00 ...
992 88.77 106.60 125.00 149.64 144.30 131.75 134.00 124.00 100.90 121.00 ...
993 130.12 139.00 127.00 127.00 121.77 142.00 121.88 127.00 120.00 130.00 ...
994 127.00 130.00 132.53 122.50 133.50 128.00 128.00 123.03 124.00 127.50 ...
995 119.18 123.57 123.77 121.28 123.00 130.29 121.35 115.13 125.25 124.94 ...

```

```

996 124.17 127.93 125.17 121.38 117.72 126.25 123.03 116.89 105.28 120.71 ...
997 118.88 118.44 121.37 124.41 113.92 119.90 115.96 119.96 113.01 109.92 ...
998 118.49 109.91 108.16 121.72 116.00 103.32 100.00 110.00 109.00 110.00 ...
999 114.34 95.00 85.06 102.00 107.00 115.00 116.00 112.00 111.38];
1000
1001 CCER_2023 = [ ...
1002 95.00 95.00 95.00 109.00 88.00 80.00 90.00 90.89 47.00 78.00 ...
1003 80.00 80.00 56.40 90.00 80.00 82.00 80.00 80.00 80.00 80.34 80.00 75.00 ...
1004 80.00 80.00 86.96 80.00 80.01 84.81 88.00 65.64 80.00 69.70 81.40 80.00 ...
1005 69.38 70.50 80.44 83.90 78.23 86.00 86.99 80.00 80.00 74.77 77.63 74.50 ...
1006 75.00 80.10 85.40 80.00 74.00 70.42 78.00 79.51 79.14 85.00 80.00 75.00 ...
1007 65.00 65.00 74.60 65.01 70.00 90.00 70.00 72.00 72.00 72.00 72.00];
1008
1009 n_days = length(CEA_2023);
1010
1011 g_yoy = [ ...
1012 2.0 ;
1013 5.8 ;
1014 5.9 ;
1015 8.3 ;
1016 7.4 ;
1017 6.4 ;
1018 6.5 ;
1019 7.6 ;
1020 6.8 ;
1021 5.2 ;
1022 11.6 ;
1023 8.0 ];
1024 g_yoy = g_yoy / 100;
1025
1026 month_id = zeros(n_days,1);
1027 edges = round(linspace(1, n_days+1, 13));
1028 for m = 1:12
1029 month_id(edges(m):edges(m+1)-1) = m;
1030 end
1031 elec_yoy_daily = g_yoy(month_id);
1032
1033 q_elec = quantile(elec_yoy_daily, [0.33 0.66]);
1034 q_price = quantile(CEA_2023, [0.33 0.66]);
1035 elec_low = q_elec(1);
1036 elec_high = q_elec(2);
1037 p_low = q_price(1);
1038 p_high = q_price(2);
1039
1040 state = zeros(n_days,1);
1041
1042 for t = 1:n_days
1043 e = elec_yoy_daily(t);
1044 p = CEA_2023(t);
1045 if (e <= elec_low && p <= p_low)
1046 state(t) = 1;
1047 elseif (e >= elec_high && p >= p_high)
1048 state(t) = 3;
1049 else
1050 state(t) = 2;
1051 end
1052 end
1053
1054 for s = 1:3
1055 if sum(state==s) < 5
1056 warning('State %d has too few observations, merging to middle state.', s);
1057 state(state==s) = 2;
1058 end
1059 end
1060
1061 log_ret_CEA = diff(log(CEA_2023));
1062 state_ret = state(2:end);
1063 n_state = 3;
1064 mu_A = zeros(n_state,1);
1065 sig_A = zeros(n_state,1);
1066
1067 for s = 1:n_state
1068 idx = (state_ret == s);
1069 rs = log_ret_CEA(idx);
1070 if isempty(rs)
1071 rs = log_ret_CEA;
1072 end
1073 mu_A(s) = mean(rs);
1074 sig_A(s) = std(rs);
1075 end
1076
1077 theta_daily = CCER_2023 ./ CEA_2023(1:length(CCER_2023));
1078 state_theta = state(1:length(theta_daily));
1079
1080 theta_state = zeros(n_state,1);
1081 for s = 1:n_state
1082 idx = (state_theta == s);
1083 ths = theta_daily(idx);
1084 if isempty(ths)
1085 ths = theta_daily;
1086 end
1087
```

```

1086     end
1087     theta_state(s) = mean(ths);
1088 end
1089 theta_state = max(theta_state, 0.5);
1090 theta_state = min(theta_state, 1.0);
1091
1092 P = zeros(n_state);
1093 for s = 1:n_state
1094     idx = find(state(1:end-1) == s);
1095     if isempty(idx)
1096         P(s,:) = 1/n_state;
1097     else
1098         next_s = state(idx+1);
1099         for j = 1:n_state
1100             P(s,j) = sum(next_s == j);
1101         end
1102         P(s,:) = P(s,:) / sum(P(s,:));
1103     end
1104 end
1105
1106 A_pi = [ (P' - eye(n_state)); ones(1,n_state) ];
1107 b_pi = [ zeros(n_state,1); 1 ];
1108 pi_stationary = A_pi \ b_pi; %#ok<NASGU>
1109
1110 r_annual = 0.0435;
1111 T_trade = 80;
1112 dt = 1/252;
1113 r_dt = r_annual * dt;
1114
1115 S0_CEA = CEA_2023(end);
1116 S0_CCER = CCER_2023(end);
1117 K = S0_CCER;
1118
1119 n_paths = 20000;
1120
1121 n_plot = 5;
1122 CEA_path_plot = zeros(T_trade+1, n_plot);
1123 CCER_path_plot = zeros(T_trade+1, n_plot);
1124 Regime_path_plot = zeros(T_trade+1, n_plot);
1125
1126 payoff = zeros(n_paths,1);
1127
1128 rng(1234);
1129
1130 for pidx = 1:n_paths
1131     cur_s = state(end);
1132     S_A = S0_CEA;
1133     S_C = S0_CCER;
1134
1135     if pidx <= n_plot
1136         CEA_path_plot(1,pidx) = S_A;
1137         CCER_path_plot(1,pidx) = S_C;
1138         Regime_path_plot(1,pidx) = cur_s;
1139     end
1140
1141     for t = 1:T_trade
1142         cur_s = draw_next_state(cur_s, P);
1143         sig = sig_A(cur_s);
1144         dW = sqrt(dt)*randn;
1145         mu_rn = r_annual - 0.5*sig^2;
1146         S_A = S_A * exp(mu_rn*dt + sig*dW);
1147         theta = theta_state(cur_s);
1148         eps_c = 0.10*sqrt(dt)*randn;
1149         S_C = theta * S_A * exp(eps_c);
1150
1151         if pidx <= n_plot
1152             CEA_path_plot(t+1,pidx) = S_A;
1153             CCER_path_plot(t+1,pidx) = S_C;
1154             Regime_path_plot(t+1,pidx) = cur_s;
1155         end
1156     end
1157     payoff(pidx) = max(S_C, K);
1158 end
1159
1160 PV_CCER_value = exp(-r_dt*T_trade) * mean(payoff);
1161
1162 time_vec = 0:T_trade;
1163
1164 figure('Name','Regime-switching GBM: CEA/CCER sample paths','Color','w','Position',[100 100 900 420]);
1165 hold on;
1166
1167 for i = 1:n_plot
1168     plot(time_vec, CEA_path_plot(:,i), '-', 'LineWidth',1.4,'Color',[0 0.447 0.741]);
1169     plot(time_vec, CCER_path_plot(:,i), '-', 'LineWidth',1.4,'Color',[0.85 0.325 0.098]);
1170 end
1171
1172 ymax_all = max([CEA_path_plot(:,1); CCER_path_plot(:,1)]);
1173 ymin_all = min([CEA_path_plot(:,1); CCER_path_plot(:,1)]);
1174 ylim([ymin_all*0.98, ymax_all*1.02]);
1175

```

```

1176 reg_path = Regime_path_plot(:,1);
1177
1178 colors = [0.9 0.95 1.0;
1179     0.9 1.0 0.9;
1180     1.0 0.9 0.9];
1181
1182 for t = 1:T_trade
1183     s = reg_path(t);
1184     x_rect = [t-0.5, t+0.5, t+0.5, t-0.5];
1185     y_rect = [ymin_all*0.98, ymin_all*0.98, ymax_all*1.02, ymax_all*1.02];
1186     patch(x_rect, y_rect, colors(s,:), 'EdgeColor','none','FaceAlpha',0.18);
1187 end
1188
1189 for i = 1:n_plot
1190     plot(time_vec, CEA_path_plot(:,i), '-','LineWidth',1.4,'Color',[0.447 0.741]);
1191     plot(time_vec, CCER_path_plot(:,i), '--','LineWidth',1.4,'Color',[0.85 0.325 0.098]);
1192 end
1193
1194 xlabel('Trading day');
1195 ylabel('Price (CNY)');
1196 title('Sample paths of CEA (solid) and CCER (dashed) under regime-switching GBM');
1197 grid on;
1198 xlim([0 T_trade]);
1199 legend({'CEA paths','CCER paths'},'Location','northwest');
1200
1201 hold off;
1202
1203 S0_grid = linspace(80, 160, 25);
1204 T_grid = 10:10:80;
1205 nS = length(S0_grid);
1206 nT = length(T_grid);
1207
1208 n_path_small = 15000;
1209
1210 K_base = CCER_2023(end);
1211 theta_mid = theta_state(2);
1212 alpha_follow = 0.3;
1213
1214 rng(5678);
1215
1216 S_samples = zeros(nS*nT,1);
1217 T_samples = zeros(nS*nT,1);
1218 P_samples = zeros(nS*nT,1);
1219 idx_sample = 0;
1220
1221 for iT = 1:nT
1222     TT = T_grid(iT);
1223     disc = exp(-r_dt*TT);
1224     for iS = 1:nS
1225         idx_sample = idx_sample + 1;
1226         S0a = S0_grid(iS);
1227         K2 = K_base + alpha_follow * theta_mid * (S0a - S0_CEA);
1228         payoff2 = zeros(n_path_small,1);
1229         for pidx = 1:n_path_small
1230             cur_s = state(end);
1231             Sa = S0a;
1232             Sc = theta_state(cur_s) * Sa;
1233             for t = 1:TT
1234                 cur_s = draw_next_state(cur_s, P);
1235                 sig = sig_A(cur_s);
1236                 dW = sqrt(dt)*randn;
1237                 mu_rn = r_annual - 0.5*sig^2;
1238                 Sa = Sa * exp(mu_rn*dt + sig*dW);
1239                 theta = theta_state(cur_s);
1240                 eps_c2 = 0.10*sqrt(dt)*randn;
1241                 Sc = theta * Sa * exp(eps_c2);
1242             end
1243             ScT = Sc;
1244             payoff2(pidx) = max(ScT, K2);
1245         end
1246         price_ij = disc * mean(payoff2);
1247         S_samples(idx_sample) = S0a;
1248         T_samples(idx_sample) = TT;
1249         P_samples(idx_sample) = price_ij;
1250     end
1251 end
1252
1253 [SG_orig, TG_orig] = meshgrid(S0_grid, T_grid);
1254 Price_surface = griddata(S_samples, T_samples, P_samples, SG_orig, TG_orig, 'linear');
1255
1256 figure('Name','CCER value surface: discounted E[max(CCER_T, K2)] (no extra smoothing)',...
1257     'Color','w','Position',[150 150 900 620]);
1258
1259 surf(SG_orig, TG_orig, Price_surface);
1260 xlabel('Initial CEA price S_0^A (CNY)', 'FontSize', 11);
1261 ylabel('Maturity T (trading days)', 'FontSize', 11);
1262 zlabel('Discounted E[ max(CCER_T, K_2) ] (CNY)', 'FontSize', 11);
1263 title('CCER value surface under regime-switching GBM: discounted E[max(CCER_T, K_2)]', 'FontSize', 12);
1264 shading interp;
1265 colormap(parula);

```

```

1266 colorbar;
1267 grid on;
1268 view(135, 30);
1269
1270 hold on;
1271 [~, idx_T40] = min(abs(T_grid - 40));
1272 plot3(S0_grid, T_grid(idx_T40)*ones(1,nS), Price_surface(idx_T40,:), ...
1273 'k','LineWidth',2);
1274 text(S0_grid(end), T_grid(idx_T40), Price_surface(idx_T40,end), ...
1275 'Slice at T \approx 40','Color','k','FontSize',10);
1276 hold off;
1277
1278 printf('===== Regime-Switching CCER Valuation (E[max(CCER_T, K)]) =====\n');
1279 printf('Risk-free annual rate r : %.4f\n', r_annual);
1280 printf('Simulation horizon (T_trade): %d trading days\n', T_trade);
1281 printf('Time step dt (in years) : 1/252\n\n');
1282
1283 printf('--- Figure 1: Sample paths under regime-switching GBM ---\n');
1284 printf('Initial CEA price S0^A : %.2f CNY\n', S0_CEA);
1285 printf('Initial CCER price S0^C : %.2f CNY\n', S0_CCER);
1286 printf('Regimes (1=low, 2=mid, 3=high) are inferred from 2023 data.\n');
1287 printf('The figure shows %d simulated CEA (solid) and CCER (dashed) paths,\n', n_plot);
1288 printf('with colored background bands indicating regime switches over time.\n');
1289 printf('These paths illustrate how CCER prices co-move with CEA prices\n');
1290 printf('and how different regimes (low/medium/high demand and price) affect\n');
1291 printf('the joint evolution of the two carbon assets.\n\n');
1292
1293 printf('--- Single-maturity CCER value at T = %d trading days ---\n', T_trade);
1294 printf('Guarantee level K (per unit CCER) : %.2f CNY\n', K);
1295 printf('Number of Monte Carlo paths (T = %d) : %d\n', T_trade, n_paths);
1296 printf('Discounted E[ max(CCER_T, K) ] (per unit) : %.4f CNY\n\n', PV_CCER_value);
1297
1298 printf('--- Figure 2: CCER value surface on the original (S0^A, T) grid ---\n');
1299 printf('Grid of initial CEA prices S0^A : from %.2f to %.2f CNY (%d points)\n', ...
1300 min(S0_grid), max(S0_grid), nS);
1301 printf('Grid of maturities T : from %d to %d trading days (%d points)\n', ...
1302 min(T_grid), max(T_grid), nT);
1303 printf('Monte Carlo paths per (S0^A, T) grid point: %d\n', n_path_small);
1304 printf('K2 is defined as K_base + alpha_follow * theta_mid * (S0^A - S0_CEA).\n');
1305 printf('where K_base = %.2f, alpha_follow = %.2f, theta_mid = %.4f.\n');
1306 K_base, alpha_follow, theta_mid);
1307 printf('This breaks the nearly linear dependence on S0^A while preserving\n');
1308 printf('the overall guarantee-contract structure E[max(CCER_T, K2)].\n');
1309 printf('The 3D surface is plotted directly on this original grid without\n');
1310 printf('any additional smoothing beyond the basic griddata interpolation.\n');
1311 printf('-----\n');
1312
1313 end
1314
1315 function next_s = draw_next_state(cur_s, P)
1316 prob = P(cur_s,:);
1317 u = rand;
1318 cumprob = cumsum(prob);
1319 next_s = find(u <= cumprob, 1, 'first');
1320 if isempty(next_s)
1321     next_s = cur_s;
1322 end
1323 end
1324

```